جـــامـعـة الـــشـرق الأوسـط
MIDDLE EAST UNIVERSITY
Amman - Jordan

Computational and Experimental Evaluation of Vanillin–Thiosemicarbazone as a Potential Inhibitor of SARS-CoV-2 3CL-protease

Maizr Ahmad A. Alshammari

Supervised by
Dr. Mohamed Jamal Saadh

This Thesis was Submitted in Fulfillment of the Requirements for the Master's Degree in Pharmaceutical Sciences at Middle East University

December, 2025

جـــامـعـــة الـــشـرق الأوسـط
MIDDLE EAST UNIVERSITY
Amman - Jordan

التقييم الحاسوبي والتجريبي لمركب فانيلين–ثيوسيميكاربازون كمثبط محتمل لإنزيم البروتياز الرئيسي (3 CL–protease) لفيروس كورونا المستجد

إعداد

ميزر احمد عبد الله الشمري

إشراف

الدكتور محمد جمال سعادة

قدّمت هذه الرسالة استكمالًا لمتطلّبات الحصول على درجة الماجستير في العلوم الصيدلانية في جامعة الشرق الأوسط

ديسمبر، 2025

Thesis Committee Decision

This thesis, titled **"Computational and Experimental Evaluation of Vanillin–Thiosemicarbazone as a Potential Inhibitor of SARS-CoV-2 3CL-protease"** by researcher **Maizr Ahmad A. Alshammari** and was successfully defended and approved on 28-12-2025.

Examination Committee Members

No.	Name	Title	Place	Signature
1	Dr. Mohammad Jamal Saadeh	Supervisor	Middle East University	.....
3	Dr. Israa Hamed Al-Ani	Internal Member and Committee Head	Middle East University	.....
4	Dr. Noor Mohsen Nasser	Internal Member	Middle East University	.....
5	Prof. Dr. Ahmed Abdulaziz Saad	External Member	Jerash University	.....

Authorization

I, **Maizer Ahmad Alshammary**, authorize Middle East University to provide copies of my thesis on paper and electronically, in whole or in part, to libraries, organizations, bodies, and institutions concerned with scientific research and studies upon request.

Name: MAIZR AHMAD A. ALSHAMMARI

Date: 28/12/ 2025.

Signature:

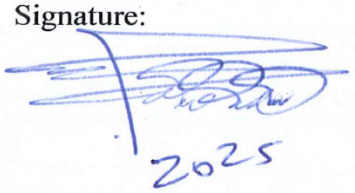

Acknowledgement

At the beginning, I thank **Allah**, who granted me the strength and opportunity to live, learn, and complete this work.

Gratefully, I would like to thank **Dr. Mohamed Saadh**, Associate Professor of Biochemistry and Molecular Biology, Faculty of Pharmacy, Middle East University, Jordan, for not only suggesting the research topic and providing me with all the laboratory facilities, but also for his invaluable supervision, constructive revision, continuous advice, and expert guidance throughout this work. I am deeply grateful for his support.

My heartfelt thanks go to the staff of the laboratory for their technical support and assistance, and to my colleagues and lab mates for their cooperation, encouragement, and the positive research environment they helped create.

Finally, I extend my deepest gratitude to my family for their patience, love, and unwavering support throughout this journey. Their prayers and encouragement were a constant source of strength.

MAIZR ALSHAMMARI

2025

Dedication

I dedicate this work to…

To the memory of **my beloved father**, may God have mercy on him.

To my beloved **mother**, the heart of our home and the source of endless compassion. Your prayers, encouragement, and gentle reassurance have carried me through every moment of doubt and fatigue. I feel your love surrounding me and guiding my steps every day. I dedicate this work to you as a small tribute to a love that gives without ever asking for anything in return.

My loving **wife**, my true partner in every season of life. You stood by me with remarkable patience, understanding, and constant support, turning difficult days into manageable ones. This dedication is for you—because your presence made this journey possible and meaningful.

My precious **children**, my greatest joy and strongest motivation. You remind me why effort matters and why dreams are worth pursuing. I dedicate this work to you in the hope that it inspires you to believe in yourselves and to chase your ambitions with courage and integrity.

My dear brothers, my lifelong companions and steady support. Your encouragement, generosity, and presence have been a source of comfort and strength throughout this journey. I dedicate this achievement to you with heartfelt appreciation and love.

MAIZR ALSHAMMARI
2025

Table of Contents

List of Tables

List of Figures

List of Appendices

List of Abbreviations

Abbreviation	Full Term
3CL-protease	3-Chymotrypsin-Like Protease (main protease of SARS-CoV-2)
4PL	Four-Parameter Logistic (model)
ATR	Attenuated Total Reflectance
COVID-19	Coronavirus Disease 2019
DMSO	Dimethyl Sulfoxide
FRET	Förster (Fluorescence) Resonance Energy Transfer
FT-IR	Fourier-Transform Infrared (spectroscopy)
GC-376	GC-376, a 3CL-protease inhibitor used as reference/positive control
IC_{50}	Half-Maximal Inhibitory Concentration
PDB	Protein Data Bank
SARS-CoV-2	Severe Acute Respiratory Syndrome Coronavirus 2
SBDD	Structure-Based Drug Design
VTSC	Vanillin–Thiosemicarbazone

Computational and Experimental Evaluation of Vanillin–*Thiosemicarbazone* as a Potential Inhibitor of SARS-CoV-2 3CL-protease

Prepared by
Maizr Ahmad A. Alshammari
Supervised by
Mohamed Jamal Saadh

Abstract

Introduction: SARS-CoV-2 3CL-protease is a key viral enzyme required for cleaving the polyprotein into functionally active proteins, making it an important target for small-molecule antiviral drug development. Vanillin is a safe phenolic compound with diverse biological activities, while thiosemicarbazide are a well-known antiviral and metal-chelating pharmacophore. Combining these two moieties in a single hybrid scaffold is expected to enhance their binding to the 3CL-protease active site and thereby improve inhibitory potency. **Objective:** The integrated molecular docking and in vitro enzyme inhibition work was used to synthesis and characterize Vanillin -Thiosemicarbazone (VTSC) and assess binding affinity and inhibiting effect against SARS-CoV-2 3CL-protease. **Results:** VTSC was achieved by Schiff base condensation of vanillin with thiosemicarbazide, validated by spectroscopic studies. Molecular docking with SARS-CoV-2 3CL-protease revealed that VTSC had the highest docking score (–4.99 kcal/mol) in comparison to vanillin (–4.764 kcal/mol) and thiosemicarbazide (–3.311 kcal/mol) and generated a more complex network of hydrogen-bond/hydrophobic interactions in the substrate-binding pocket. A recombinant fluorometric 3CL-protease assay revealed all three compounds to inhibit enzyme activity in a dose-dependent manner but differing in potency: thiosemicarbazide was a weak inhibitor $IC_{50} \approx 191$ μM, vanillin moderate activity $IC_{50} \approx 42.0$ μM and VTSC strongest inhibition $IC_{50} \approx 28.7$ μM. Therefore, it is suggested that when a thiosemicarbazone pharmacophore was incorporated into the vanillin core in this same assay, the potency of the compound was improved by an approximate 1.5-fold compared to vanillin alone. **Conclusions:** The data show that Vanillin–Thiosemicarbazone is a small, easily synthesized molecule with improved predicted binding and higher in vitro inhibition of SARS-CoV-2 3CL-protease than its parent compounds, making it a promising template for designing more potent COVID-19 drug candidates.

Keywords: SARS-CoV-2; 3CL-protease inhibitor; Vanillin–Thiosemicarbazone (VTSC); Fluorometric enzyme assay; Molecular docking; Antiviral drug discovery.

التقييم الحاسوبي والتجريبي لمركب فانيلين–ثيوسيميكاربازون كمثبط محتمل لإنزيم البروتياز الرئيسي (3CL-protease) لفيروس كورونا المستجد

اعداد الطالب
ميزر احمد الشمري
تحت اشراف
د. محمد جمال سعادة

الملخص

المقدمة: يُعد إنزيم البروتياز الرئيسي لفيروس SARS-CoV-2 (3CL-protease) أحد العناصر الأساسية في دورة تكاثر الفيروس، إذ يلعب دورًا محوريًا في شطر البروتين متعدد الوحدات إلى بروتينات وظيفية نشطة، مما يجعله هدفًا مهمًا لتطوير أدوية مضادة للفيروسات صغيرة الجزيء. يُعرف الفانيلين بأنه مركب فينولي آمن يمتلك أنشطة حيوية متعددة، في حين تُعد مركبات الثايوسيميكاربازون من الحوامل الدوائية المعروفة بفعاليتها المضادة للفيروسات وقدرتها على الارتباط بالمعادن. ومن المتوقع أن يؤدي دمج هذين الجزأين البنيويين في هيكل هجين واحد إلى تعزيز الارتباط بالموقع النشط لإنزيم CL-protease 3وبالتالي تحسين القدرة التثبيطية. **الهدف:** هدفت هذه الدراسة إلى تصنيع وتوصيف مركب فانيلين–ثايوسيميكاربازون(VTSC) ، وتقييم ألفته الارتباطية وتأثيره المثبط لإنزيم CL-protease 3باستخدام تقنيات الالتحام الجزيئي (molecular docking) واختبارات التثبيط الإنزيمي في المختبر. **النتائج:** تم تحضير مركب VTSCبنجاح من خلال تفاعل تكاثف قاعدة شيف بين الفانيلين والثايوسيميكاربازيد، وتم تأكيد تركيبه بواسطة التحاليل الطيفية. أظهرت دراسات الالتحام الجزيئي أن مركب VTSC حقق أعلى طاقة ارتباط مع إنزيم CL-protease 3مقارنةً بالفانيلين والثايوسيميكاربازيد، كما كوّن شبكة أكثر تعقيدًا من التفاعلات الهيدروجينية والهيدروفوبية داخل جيب الارتباط الخاص بالركيزة. وبينت نتائج الاختبار الفلورومتري للإنزيم أن المركبات الثلاثة أظهرت تثبيطًا معتمدًا على التركيز، مع اختلاف واضح في الفعالية؛ حيث كان الثايوسيميكاربازيد مثبطًا ضعيفًا، وأظهر الفانيلين فعالية متوسطة، بينما سجل مركب VTSC أعلى قدرة تثبيطية بقيمة IC_{50} أقل. وقد أدى دمج مجموعة الثايوسيميكاربازون ضمن نواة الفانيلين إلى تحسين الفعالية التثبيطية بحوالي 1.5 مرة مقارنة بالفانيلين وحده. **الاستنتاجات:** تشير النتائج إلى أن مركب فانيلين–ثايوسيميكاربازون هو جزيء صغير سهل التحضير، يتمتع بألفة ارتباط محسّنة وقدرة تثبيطية أعلى لإنزيم CL-3 proteaseمقارنة بالمركبات الأم. وتبرز هذه الخصائص إمكانيته كقالب واعد لتصميم وتطوير مركبات دوائية أكثر فعالية لمكافحة مرض كوفيد-19.

الكلمات المفتاحية :SARS-CoV-2؛ مثبط إنزيم CL-protease3؛ فانيلين–ثايوسـيميكاربازون ؛ اختبار إنزيمي فلورومتري؛ الالتحام الجزيئي؛ اكتشاف الأدوية المضادة للفيروسات.

Chapter One

Background and Problem Statement

1.1 Introduction

The COVID-19, caused by the Severe Acute Respiratory Syndrome Coronavirus 2 (SARS-CoV-2), has created a need for effective antiviral agents targeting the key viral proteins involved in the replication and maturation of SARS-CoV-2. Vaccine development has been associated with much success (Lv et al., 2022). On the other hand, several antiviral agents are always in development. However, clinical and other responses to the new variants of the SARS-CoV-2 virus vary significantly. Also, there are concerns about the resistance of some of these drugs and failure of drug efficacy in some patient populations. All this highlights the extreme need for the development of new inhibitors based on simple molecular targets and simple synthetic pathways. Review articles have consistently discussed these observations (Lv et al., 2022; Razali et al., 2021).

The 3CL protease is a viral enzyme that cleaves the viral polypeptides that emerge following the genomic and sub-genomic translation of the SARS-CoV-2 virus into structural and nonstructural proteins. The 3CL-protease has an active site that is highly conserved and has few similar homologs in humans, making it a validated and attractive target for antiviral drug development. Furthermore, there are several recent small-molecule inhibitors that have been designed to inhibit it (Lv et al., 2022; Razali et al., 2021; Kronenberger et al., 2023; Kang et al., 2025). It is therefore considered a reasonable and promising approach to inhibit this protease to control SARS-CoV-2 replication.

Natural products have long contributed to the field of drug discovery and related areas. Their derivatives have played an important role in the development of medicines for human health. Such compounds often have structurally diverse scaffolds and a relatively favorable safety profile. More importantly, they exhibit an extensive range of biological activities (Arya et al., 2021). Thus we need to keep natural products and their derivatives as potential materials for drug discovery. Vanillin (or 4-hydroxy-3-methoxybenzaldehyde) is a naturally occurring compound that has been thoroughly characterized. Vanillin has antioxidant, anti-inflammatory, antimicrobial, and other beneficial actions. These actions

render vanillin an interesting scaffold in the design of a diverse number of therapeutic candidates (Arya et al., 2021; Olatunde et al., 2022; Kafali et al., 2024).

An important class of Schiff base derivatives which have shown antiviral, anti-microbial and anti-cancer activity are thiosemicarbazides and Thiosemicarbazones respectively. Many thiosemicarbazone based compounds and their metal complexes show anti-viral inhibition against various viruses. They can act as ligands for viral enzymes and nucleic acids (Czylkowska et al., 2024; Padmanabhan et al., 2017; Pacca et al., 2017). The functional groups of these ligands are electron-donating and metal-chelating, which allows for strong and flexible interactions, including with proteases (Padmanabhan et al., 2017).

The reaction of vanillin with thiosemicarbazide yields Vanillin–Thiosemicarbazone (VTSC) with phenolic, azomethine (C=N) and thiosemicarbazone functionalities coupled in one hybrid scaffold. The design may be effective in forming multiple hydrogen bonding and π–π interactions with the key residues of the catalytic pocket of 3CL-protease, thus improving its inhibitory activity when compared with parent compounds, vanillin and thiosemicarbazide (Swaminathan et al., 2023).

To date, however, there is limited experimental evidence directly assessing Vanillin–Thiosemicarbazone as an inhibitor of 3CL-protease. Currently, there's insufficient integrated studies combining molecular docking with in vitro enzyme inhibition assays to characterize its binding mode and functional effect in relation to vanillin and thiosemicarbazide.

Therefore, this study is designed to synthesize and characterize Vanillin–Thiosemicarbazone, evaluate its predicted binding affinity toward 3CL-protease using molecular docking, and investigate its in vitro inhibitory activity against 3CL-protease using a standardized fluorometric assay, with direct comparison to vanillin and thiosemicarbazide.

1.2 Study Problem

1.3 Study Questions

In this study we aim to answer the following questions:

1. What is the anticipated binding affinity and interaction profile of VTSC with the active site of 3CL-protease determined by molecular docking compared with both vanillin and thiosemicarbazide?

2. Does VTSC has a significant, dose-dependent inhibitory effect on 3CL-protease activity in vitro?

3. What are the differences between the IC_{50} values of Vanillin–Thiosemicarbazone, vanillin and thiosemicarbazide under identical experimental conditions?

4. To what extent do the molecular docking predictions correlate with the experimental inhibitory effects of Vanillin–Thiosemicarbazone (VTSC) against 3CL-protease?

1.4 Study Hypotheses

The study is guided by the following null hypotheses:

• H_{01}: There is no significant difference in the predicted binding affinity of VTSC toward 3CL-protease compared with vanillin and thiosemicarbazide.

• H_{02}: VTSC does not produce a significant inhibitory effect on 3CL-protease activity in vitro.

• H_{03}: There is no significant difference between the IC_{50} value of VTSC and the IC_{50} values of vanillin and thiosemicarbazide under identical experimental conditions.

• H_{04}: There is no meaningful agreement between the molecular docking predictions and the in vitro inhibitory activity observed for VTSC against 3CL-protease.

1.5 Study Objectives

General Objective

To evaluate VTSC as a potential inhibitor of 3CL-protease through integrated molecular docking and in vitro enzyme inhibition approaches.

Specific Objectives

- To synthesize and characterize VTSC.
- To conduct molecular docking studies of VTSC, designed using the theory of hybridization and crystal structures of vanillin, and thiosemicarbazide.
- To evaluate the dose-dependent inhibitory effect of VTSC on 3CL-protease activity using a fluorometric enzyme inhibition assay and determine its IC_{50} value.
- To compare the inhibitory activity and IC_{50} values of VTSC with those of vanillin and thiosemicarbazide under the same experimental conditions.
- To examine the consistency between molecular docking outcomes and the experimental inhibition profiles of VTSC.

1.6 Study Importance

Scientific Importance

A study regarding the synthesis, structural characterization, and inhibitory evaluation of VTSC as a 3CL-protease inhibitor will be presented. Combining molecular docking with in vitro enzyme assays, the system allows rational decision-making to be made about how to design and test small molecules as inhibitors against viral proteases (Lv et al., 2022; Kronenberger et al., 2023; Kang et al., 2025).

The VTSC has been made from uncomplicated low cost precursors and may as a lead structure be of interest for further elucidation and optimization. Positive results might promote the use of structurally related analogues to obtain anti-coronaviral agents, especially in low-resource settings.

Exhibits a consistent approach of synthesis, characterization, molecular docking, and in vitro enzyme inhibition that can be utilized to screen and validate other small molecule candidates against 3CL-protease and other similar targets.

1.7 Study Limitations

Limitations to Interpretation of the Results

1. These in vitro assays are based on 3CL-protease, and the cell uptake, metabolic stability, protein binding or full antiviral activity are not considered for these *in vitro* models.
2. Molecular docking provides an approximate description of binding affinity and interaction modes based on static structural models and scoring functions; it does not fully account for protein flexibility, solvent dynamics, or all possible conformational states. The paper has presented only one hybrid form that comprises a single hybrid molecule VTSC and two parent compounds and does not include structurally equivalent derivatives or metal complexes.
3. The cytotoxicity, selectivity index and more general safety or pharmacokinetic testing is not included in this thesis so interpretations are limited to action at enzyme level.

1.8 Operational Definitions

1. SARS-CoV-2

   The human coronavirus producing Coronavirus Disease 2019 (COVID-19), that is the virus responsible for this study's source of viral 3CL-protease.

2. 3CL-protease

   The SARS-CoV-2 3-chymotrypsin-like cysteine protease is responsible for proteolytic cleavage of viral polyproteins (pp1a and pp1ab) into non-structural proteins which are essential for viral replication. In this thesis, it is the specific molecular target for inhibition.

3. Vanillin

   4-hydroxy-3-methoxybenzaldehyde; a phenolic aldehyde of interest in these

studies as a bioactive parent compound and as the aldehydic precursor for Vanillin–Thiosemicarbazone synthesis. It is also tested as a reference compound in molecular docking and in vitro inhibition assays.

4. Thiosemicarbazide

   A nitrogen and sulfur containing compound with thiosemicarbazide functional group. For the purpose of this thesis, this compound is used as a precursor for the formation of thiosemicarbazone and considered as a reference compound alongside Vanillin–Thiosemicarbazone.

5. Vanillin–Thiosemicarbazone (VTSC)

   It's Schiff base [thiosemicarbazone derivative], made by condensation of vanillin with thiosemicarbazide. In this thesis, it represents the principal test compound and will be synthesized and characterized as part of a study on 3CL-protease inhibitors.

6. Molecular Docking

   A computational approach in this study to predict the binding pose and estimate the relative binding affinity of Vanillin–Thiosemicarbazone, vanillin and thiosemicarbazide within the active site of 3CL-protease by means of a predetermined docking protocol.

7. In Vitro Enzyme Inhibition Assay

   A fluorometric assay based on recombinant 3CL-protease and a specific fluorogenic substrate, employed in this thesis to measure the inhibitory effect of the tested compounds on 3CL-protease activity at different concentrations.

8. IC_{50} (Half-Maximal Inhibitory Concentration)

   The concentration of a tested compound inducing 50% inhibition of 3CL-protease enzymatic activity under the specified experimental conditions used in this thesis.

Chapter Two

Theoretical Framework and Previous Studies

2.1 Theoretical Framework

2.1.1 SARS-CoV-2 3CL-Protease as a Therapeutic Target

Replication of SARS-CoV-2 relies on proteolytic cleavage of the viral polyproteins pp1a and pp1ab into a series of non-structural proteins which constitute the replication–transcription complex (Kang et al., 2025). This cleavage is facilitated primarily by the 3CL-protease, a cysteine protease with a conserved His41–Cys145 catalytic dyad as well as a distinct substrate-binding cleft. The 3CL-protease is essential for viral replication. Due to the absence of closely related human homologs, 3CL-protease is considered a highly selective antiviral target according to structural and functional studies (Lv et al., 2022; Razali et al., 2021; Kronenberger et al., 2023; Kang et al., 2025).

The successful clinical development of direct 3CL-protease inhibitors, together with ongoing discovery of new scaffolds, strongly validate the enzyme as a central point of intervention and continue to drive further investigation for a relatively straightforward and synthetically acceptable small molecule compound to efficiently block the activity of 3CL-protease (Lv et al., 2022; Razali et al., 2021; Kronenberger et al., 2023; Kang et al., 2025). The current thesis is positioned within this framework, particularly in the design and characterization of VTSC against 3CL-protease.

2.1.2 Structure-Based Drug Design Targeting Viral Proteases

In structure-based drug design (SBDD), high-resolution structural information of target proteins is used to guide ligand selection and optimization. For 3CL-protease, the corresponding crystal structures define essential subsites (S1, S1′, S2, S4) and the residues His41, Cys145, His163, His164, Glu166, and Gln189 are highlighted as critical for substrate and inhibitor recognition. Rationally designed inhibitors typically establish a combination of hydrogen bonding, hydrophobic contacts, and π–π interactions within these regions (Lv et al., 2022; Razali et al., 2021; Kronenberger et al., 2023; Kang et al., 2025).

In this paradigm, compact non-peptidic ligands are of special interest because they offer potential advantages in terms of oral bioavailability and synthetic simplicity, and lowered development costs (Xiao et al., 2024; Braconi et al., 2025). As a result, the present study is grounded in the structural perspective and uses VTSC, vanillin, and thiosemicarbazide as docking agents into the 3CL-protease active site for visualizing binding modes and interpretation of the experimental inhibition data.

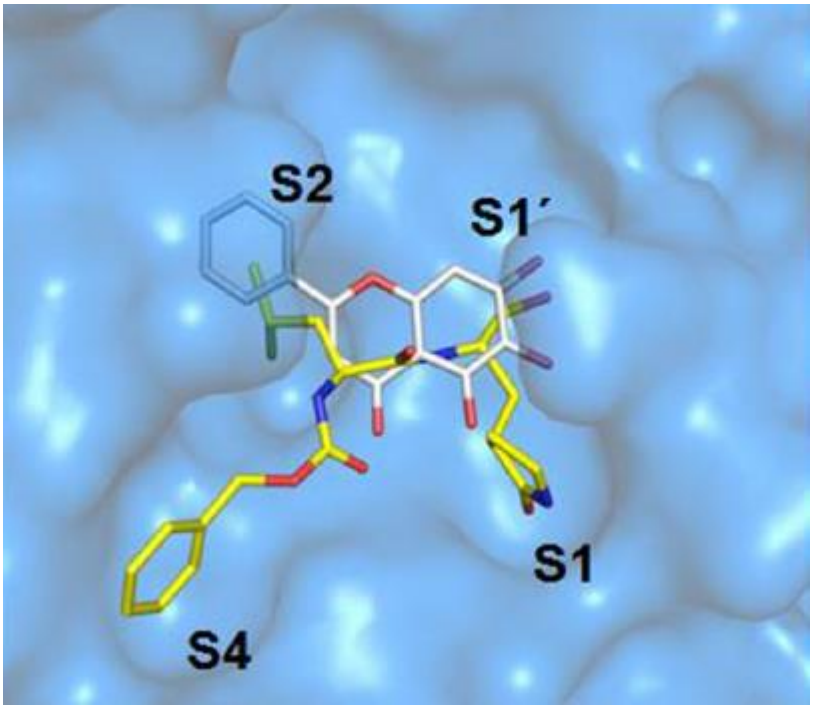

Scheme 1. Schematic illustration of the binding orientation of the ligand in the catalytic cleft of SARS-CoV-2 3CL-protease, showing its distribution across the S1, S1′, S2, and S4 substrate-binding pockets.

2.1.3 Vanillin: Chemical and Biological Profile

Vanillin (4-hydroxy-3-methoxybenzaldehyde) is the principal flavor component of vanilla but is increasingly recognized as a bioactive small molecule. Reports showed it can reduce inflammation and microbial activity. It may also prevent cancer and nerve cell damage (Arya et al., 2021; Olatunde et al., 2022; Kafali et al., 2024). Vanillin, which is generally regarded as safe (GRAS) is used in food and pharmaceutical application (Arya et al., 2021; Olatunde et al., 2022; Kafali et al., 2024).

Structurally, vanillin possesses a phenolic hydroxyl group, a methoxy group, and an aldehyde function, enabling hydrogen bonding, electron donation, and facile formation of Schiff bases. These properties make vanillin a useful pharmacophoric core for generating hybrid molecules (Arya et al., 2021; Olatunde et al., 2022; Kafali et al., 2024). In this thesis, vanillin serves as (i) a parent compound evaluated against 3CL-protease and (ii) the aldehydic precursor used in the synthesis of VTSC.

2.1.4 Thiosemicarbazide and Thiosemicarbazones as Bioactive Scaffolds

Thiosemicarbazones are a versatile class of Schiff bases containing the C=N–NH–C(S)–NH fragment, whereas thiosemicarbazides serve as their precursors. Due to its motif, extensive hydrogen bonding and coordination to metal centers have been accomplished, and it is thought to possess many biological effects, including antimicrobial, antiviral, antiparasitic along with anticancer effects (Czylkowska et al., 2024; Padmanabhan et al., 2017; Pacca et al., 2017). Thus the importance of having such small structural adjustments on thiosemicarbazone structure on potency and selectivity can be underscored through recent assessments, which illustrates its possible usefulness as a design starting point in the field of medicinal chemistry (Czylkowska et al., 2024; Padmanabhan et al., 2017; Pacca et al., 2017). Hence, applying this pharmacophore in a vanillin-based hybrid such as VTSC could feasibly be justified through targeting of enzymes such as 3CL-protease.

2.1.5 Rationale for VTSC

The VTSC is obtained by condensation of vanillin with thiosemicarbazide, generating a hybrid ligand that integrates three key features:

1. An aromatic phenolic ring, enabling π–π stacking and hydrogen bonding;
2. An azomethine (C=N) linkage, commonly associated with enhanced biological activity in Schiff bases;
3. A thiosemicarbazone moiety, providing additional donor atoms and polar interaction sites. It is anticipated that the structural features of VTSC will enhance the density and complementarity of its interactions within the 3CL-protease

binding pocket, potentially resulting in stronger and more stable binding than that of vanillin or thiosemicarbazide alone. This thesis theoretical framework is therefore based on assessing whether this rational design is manifest in: (i) advantageous docking poses and interaction profiles, and (ii) measurable inhibition of 3CL-protease in vitro (Jin et al., 2020).

2.1.6 Molecular Docking and in Vitro Enzyme Inhibition as Complementary Approaches

Molecular docking provides prediction about orienting the candidate ligands in the 3CL-protease active site and comparative binding affinity estimates. Docking is the most frequently applied first-line indicator in current antiviral studies and prior to biochemical tests (Kronenberger et al., 2023; Kang et al., 2025). In vitro fluorometric 3CL-protease inhibition assays, with recombinant enzyme and fluorogenic substrates, permit the direct determination of residual enzymatic capacity and calibration of IC_{50} values from a range of concentration levels (BPS Bioscience, n.d.; Kuzikov et al., 2021; Le Berre et al., 2022). Interpreting inhibition curves together with docking predictions gives a consistent view of how well a compound could potentially inhibit 3CL-protease (Kuzikov et al., 2021; Kronenberger et al., 2023). This integrated approach in assessing VTSC's comparability with vanillin and thiosemicarbazide is explicitly adopted in the present thesis.

2.2 Previous Studies

2.2.1 Studies on SARS-CoV-2 3CL-protease Inhibitors

Substantial attention has been devoted to the search for small-molecule inhibitors of 3CL-protease since the advent of COVID-19. Studies on structure and mechanism have characterized the architecture of the catalytic site and major interactions defining the inhibitor-binding properties and allowed for rational development and optimization of covalent and non-covalent ligands (Lv et al., 2022; Razali et al., 2021; Kronenberger et al., 2023; Kang et al., 2025). In recent reviews, the progress towards the recognition of peptidomimetic and non-peptidic 3CL-protease inhibitors is summarized including those that have reached clinical application or are

in advanced development stages, and resistance-associated mutations have also been identified, and need for structurally diverse backup candidates is also pointed out (Lv et al., 2022; Razali et al., 2021; Kronenberger et al., 2023; Kang et al., 2025). Taken together, these studies reinforce that 3CL-protease remains a priority antiviral target and are a substantial reason for further investigation of additional scaffolds, including relatively simple hybrids like VTSC.

2.2.2 Studies on Vanillin and Its Derivatives

Many articles have repositioned vanillin from a flavoring compound to a biologically active small molecule with antioxidant, anti-inflammatory, antimicrobial, and cytoprotective properties (Arya et al., 2021; Olatunde et al., 2022; Kafali et al., 2024). Subsequent studies have extended research on vanillin-derived Schiff bases and other derivatives and indicated that derivatization of the vanillin core can have a significant impact on its physicochemical properties and biological actions (Arya et al., 2021; Olatunde et al., 2022; Kafali et al., 2024). These works highlight the potential of vanillin as a modular scaffold for designing new ligands. However, vanillin-based thiosemicarbazones specifically targeting 3CL-protease have not been systematically explored.

Most significant is the clinical relevance of targeting SARS-CoV-2 3CL-protease, proven with the approval of nirmatrelvir/ritonavir (Paxlovid), a covalent 3CL-protease inhibitor that showed significant clinical efficacy in slowing disease progression of high-risk COVID-19 patients The New England Journal of Medicine (Hammond et al., 2022). Researchers have made multiple attempts to find more design diversity various designed non-covalent inhibitors have been developed S-217622 is a late-stage clinical candidate that is an orally bioavailable 3CL-protease inhibitor that has been granted emergency approval in Japan Its development showcases an interest in different scaffold classes, to bypass resistance and optimize antiviral activity Journal of Medicinal Chemistry (Unoh et al., 2022)

2.2.3 Studies on Thiosemicarbazones as Antiviral and Enzyme Inhibitors

Thiosemicarbazones are known as bioactive ligands with antimicrobial and anticancer activity (Czylkowska et al., 2024). A recent systematic review contains a vast amount of data providing excellent activity for many thiosemicarbazone based compounds and indicates the capacity of thiosemicarbazone targeting in a variety of biological systems (Czylkowska et al., 2024). Several recent works integrate synthesis, docking, and biological evaluation of thiosemicarbazone derivatives against viral or enzymatic targets, corroborating the potential of this scaffold for rational antiviral development (Padmanabhan et al., 2017; Pacca et al., 2017).

2.2.4 Studies Combining Molecular Docking and in Vitro 3CL-protease Assays

The inclusion of integrated workflows that combine in silico screening with biochemical assays is now accepted as normal in 3CL-protease inhibitor discovery. Multiple studies document how molecular docking or virtual screening was used to prioritize candidates, then fluorometric 3CL-protease inhibition assays to test hits and measure IC_{50} values (Lv et al., 2022; Kronenberger et al., 2023; Kuzikov et al., 2021; Le Berre et al., 2022).

These methods have been used to identify repurposed drugs, natural products, and de novo designed compounds, which emphasizes the need to integrate predictions with experimental data (Lv et al., 2022; Kronenberger et al., 2023; Kang et al., 2025). The following methodological approach used in this work docking followed by in vitro enzyme inhibition for VTSC, vanillin, and thiosemicarbazide is fully aligned with this widely adopted screening strategy.

2.2.5 Studies on Hybrid Molecules and Schiff Bases Targeting Viral Proteases

Recent hybrid molecules and Schiff bases that incorporate pharmacophoric elements may represent inhibitors of viral proteases. The specific targeting of Schiff bases and related hybrids shows potential favorable binding for 3CL-protease and other viral enzymes, which are often advantageous thanks to synergistic effects of the

combination of functional groups (Czylkowska et al., 2024; Padmanabhan et al., 2017; Pacca et al., 2017). These findings contribute to the conceptual basis for the design of VTSC as a simple vanillin-derived metal-free hybrid with a thiosemicarbazone moiety. However, no published work has delivered a focused, side-by-side docking and in vitro characterization of VTSC against 3CL-protease.

2.2.6 Summary of Previous Studies and Research Gap

A few points can be noted in terms of the literature reviewed:

1. 3CL-protease as a target:
   SARS-CoV-2 3CL-protease is a structurally resolved, clinically validated antiviral target and remains core to small-molecule therapeutics for COVID-19 (Lv et al., 2022; Razali et al., 2021; Kronenberger et al., 2023; Kang et al., 2025).
2. Vanillin as a scaffold:
   Vanillin is a safe, bioactive, and easily synthetic scaffold for the synthesis of new derivatives (Arya et al., 2021; Olatunde et al., 2022; Kafali et al., 2024).
3. Bioactive thiosemicarbazones as ligands:
   Thiosemicarbazones have emerged as a potential class of bioactive ligands with great potential for targeting both enzymes and viral systems (Czylkowska et al., 2024; Padmanabhan et al., 2017; Pacca et al., 2017).
4. Docking for in vitro assays:
   Molecular docking assays combined with fluorometric 3CL-protease inhibition assays are broadly well-accepted and useful for assessing candidate inhibitors (Kuzikov et al., 2021; Le Berre et al., 2022).

Despite the solid basis, this specific gap is directly relevant to the present thesis: vanillin–Thiosemicarbazone (VTSC) has not been systematically developed, characterised, docked, and experimentally assessed as an inhibitor against 3CL-protease, and has not been directly compared with their respective parent compounds vanillin and thiosemicarbazide within a unified methodological framework. Filling this gap is the main contribution of this study and connects the theoretical background and previous studies directly to the research design provided in the following chapters.

Chapter Three

Materials and Methods

3.1 Reagents and Solutions

VTSC was prepared according to Section 3.1. Stock solutions of VTSC, vanillin, and thiosemicarbazide were prepared in dimethyl sulfoxide (DMSO; analytical grade) at appropriate concentrations (e.g., 10–100 mM) and stored at 4 °C in the dark. The stock solutions were immediately diluted with assay buffer to the corresponding working concentrations before use. The final DMSO concentration in all wells (including control wells) was kept at ≤1% (v/v).

The enzymatic activity of 3CL-protease was evaluated using a commercially available fluorometric 3CL-protease assay kit (e.g., 3CL Protease Assay Kit; BPS Bioscience, San Diego, CA, USA) that contains recombinant 3CL-protease, assay buffer, the fluorogenic FRET substrate DABCYL–KTSAVLQSGFRKME–EDANS, and GC-376 as a reference inhibitor. All other chemicals and solvents were of analytical grade and were used as supplied.

3.2 Synthesis of Vanillin–Thiosemicarbazone (VTSC)

VTSC was prepared by a Schiff base condensation of vanillin (4-hydroxy-3-methoxybenzaldehyde; Sigma–Aldrich, ≥99%) with thiosemicarbazide (Merck, analytical grade) in absolute ethanol. Equimolar amounts of vanillin (10 mmol) and thiosemicarbazide (10 mmol) were dissolved independently in ethanol (25 mL) under magnetic stirring, joined as a mixture, and supplemented with a few drops of glacial acetic acid (Sigma–Aldrich, ≥99.7%) as an acid catalyst. The reaction mixture was refluxed for ~2 h at 70–80 °C, where a pale-yellow precipitate formed. The reaction was then cooled to room temperature. The solid product was obtained by vacuum filtration and washed repeatedly with cold ethanol to remove unreacted starting materials, followed by crystallization from an ethanol-water mixture (1:1, v/v). Purified VTSC was obtained as pale-yellow crystals dried in a vacuum oven at 40–50 °C for 12 h and stored in a dark, airtight container until use. The synthesis

was modified slightly from the literature procedure for vanillin–thiosemicarbazone derivatives (Tokalı et al., 2023). The chemical structure of VTSC is shown in Figure 1.

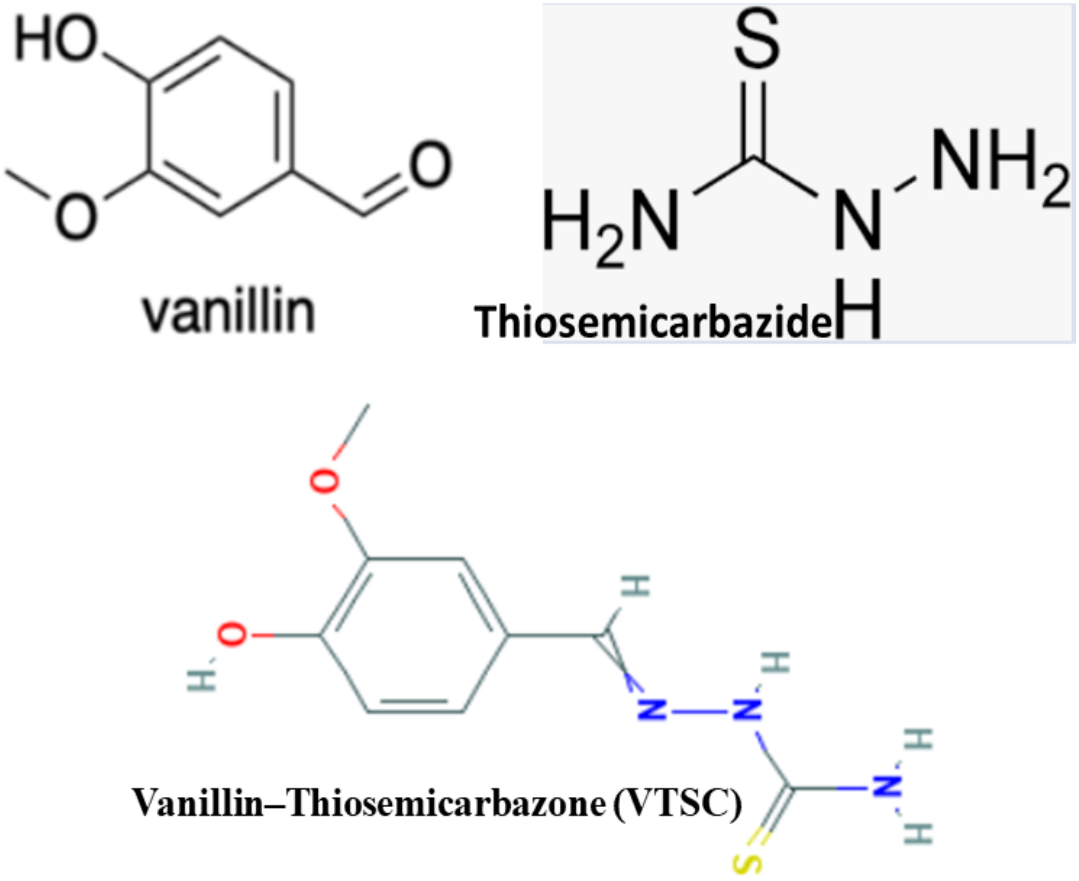

Figure 1. Chemical structure of VTSC.

3.3 FT-IR Characterization of VTSC

The functional groups of VTSC were determined by Fourier-transform infrared (FT-IR) spectroscopy. The FT-IR spectra were recorded at room temperature on a Bruker FT-IR spectrometer equipped with a diamond ATR accessory. Spectra were collected from 4000–500 cm^{-1}, with a resolution of 4 cm^{-1} and 32 co-added scans per sample. A fresh background spectrum was obtained before each analysis, and all spectra were baseline-corrected prior to analysis. Characteristic bands of ν(O–H), ν(N–H), ν(C=N) (azomethine), ν(C=S) and

aromatic ring vibrations were assigned based on data from VTSC and similar thiosemicarbazone analogues (Czylkowska et al., 2024; Swaminathan et al., 2023).

3.4 Molecular Docking of Vanillin, Thiosemicarbazide, and VTSC

Molecular docking was performed to compare the binding of vanillin, thiosemicarbazide, and VTSC to the 3CL-protease active site. The three-dimensional counterpart of the viral 3CL-protease (PDB ID: 9LVV) was selected from the Protein Data Bank because a high-resolution X-ray structure that contains co-crystallized inhibitor in catalytic cleft, the PDB ID: 9LVV is expected to show a reliable definition of active site subsites (S1/S1′/S2/S4) for docking. Protein structure was prepared by the elimination of nonessential co-crystallized ligands and crystallographic water molecules (except if they were structurally pertinent) as well as by the addition of polar hydrogens and the assignment of protonation to a state suitable for pH 7.4, most importantly the His41/Cys145 catalytic dyad. Ligand structures (vanillin, thiosemicarbazide and VTSC) are shown in 2D then converted to 3D shape, energy-minimized and assigned corresponding partial charges.

All docking was carried out using AutoDock Vina and a box with three dimensions around the 3CL-protease catalytic cleft with the S1, S1′, S2 and S4 subsites was calculated. All three ligands had the same docking settings to maintain similar performance (Zagórska et al., 2024). Several binding poses were generated for each compound (nine binding poses were generated for each ligand), resulting in the most preferred pose using predicted binding energy (kcal/mol) and orientations in the targeted active site, along with the identification of important interactions that sustain the interaction (i.e., hydrogen bonds, π–π, π–alkyl contacts, and polar interactions) with residues known to regulate substrate and inhibitor recognition. Visualization algorithms were utilized to determine the interaction between protein and ligand that allowed generating 2D interaction maps and 3D binding models to directly analyze docking profiles of vanillin, thiosemicarbazide and VTSC.

3.5 3CL-protease Inhibition Assay

Inhibition activities of VTSC, vanillin, and thiosemicarbazide on 3CL-protease were assayed using a fluorometric SARS-CoV-2 3CL-protease assay kit (BPS Bioscience, San Diego, CA, USA), with minor modifications to the manufacturer’s protocol (Froggatt et al.,

2020). Assays were carried out in black, flat-bottom 96-well microplates with a final volume of 50 µL per well.

Recombinant 3CL-protease (final amount ~90–150 ng per well, corresponding to 3–5 ng/µL in the reaction mixture, as recommended in the kit protocol) was pre-incubated at room temperature for 20–30 min with two-fold serial dilutions of the test compounds prepared in assay buffer. The DMSO concentration was kept at ≤1% (v/v) in all wells. After pre-incubation, the fluorogenic substrate DABCYL–KTSAVLQSGFRKME–EDANS was added to each well at a final concentration of 50 µM, and fluorescence intensity was measured after a 30-min incubation period (excitation 336 nm, emission 455–460 nm) using a microplate reader under conditions that maintained the reaction in the linear range.

Each concentration of the test compounds was evaluated in triplicate (n = 3). Wells containing enzyme plus vehicle (assay buffer with DMSO ≤1%) served as high-signal controls (100% enzyme activity), and GC-376 was included on plate as a positive control to demonstrate assay performance. Wells without enzyme were used as background controls. For each concentration, percent inhibition was calculated (equation 1) relative to the mean fluorescence of the vehicle control wells, after subtraction of the background signal. The experimental setup for the positive control, test inhibitor, inhibitor control, and blank is summarized in Table 1.

Percent inhibition (%) = [(vehicle control fluorescence − sample fluorescence) / (vehicle control fluorescence − blank fluorescence)] × 100……..(equation 1)

Table 1 Reaction components and volumes used in the fluorometric SARS-CoV-2 3CL-protease inhibition assay

Component	Positive Control	Test Inhibitor	Inhibitor Control	Blank
3CL Protease (3-5 ng/µl)	30 µl	30 µl	30 µl	–
Assay Buffer (with DTT)	–	–	–	30 µl
GC376 (500 µM)	–	–	10 µl	–
Test Inhibitor	–	10 µl	–	–
Diluent Solution (no inhibitor)	10 µl	–	–	10 µl
Total	**40 µl**	**40 µl**	**40 µl**	**40 µl**

3.6 Dose–Response and IC_{50} Determination

Dose–response curves for VTSC, vanillin, and thiosemicarbazide were generated by plotting percent inhibition of 3CL-protease activity versus the logarithm (base 10) of inhibitor concentration. The data were analysed using a four-parameter logistic (4PL, variable-slope) approach to obtain IC_{50} values and their 95% confidence intervals. The nonlinear regression analyses were conducted with GraphPad Prism (Version 7). San Diego, CA, USAas per standard recommendations for inhibitory concentration–response analysis (Sebaugh, 2011 & Le Berre et al., 2022). For IC_{50} reporting, only data sets that met basic quality criteria (adequate dynamic range, appropriate curve shape, and goodness-of-fit) were considered.

3.7 Statistical Analysis

All enzyme inhibition tests were carried out individually in triplicate (n = 3), and values presented as mean ± standard deviation (SD). Statistical analyses were carried out using GraphPad Prism. The study applied a one-way analysis of variance (ANOVA) along with the Tukey's test for post hoc multiple comparisons to obtain differences in inhibitory activity (either IC_{50} values or percent inhibition at selected concentrations) among VTSC, vanillin, and thiosemicarbazide. A p-value less than 0.05 is determined as statistically significant.

Chapter Four

Results

4.1 Molecular Docking

4.1.1 Vanillin

Docking data of vanillin (Figure 2) displayed a moderate binding affinity within the active site of the SARS-CoV-2 3CL-Protease (3CL-protease) with a docking score of 4.764 kcal/mol. The ligand had 2 major H-bonds with Thr26 and Gly143. The aromatic ring was located near Cys145, one of the catalytic residues, indicating some interaction with the substrate-binding pocket. The stabilizing hydroxyl and methoxy groups of vanillin stabilized the ligand through polar interactions with residues such as Asn142 and Thr25. During molecular docking investigation, it was found that although vanillin was located within the catalytic pocket, it did not provide a significant hydrogen-bond network and did not make optimal hydrophobic subpocket contacts. Thus, it may have moderate anti-3CL-protease potential.

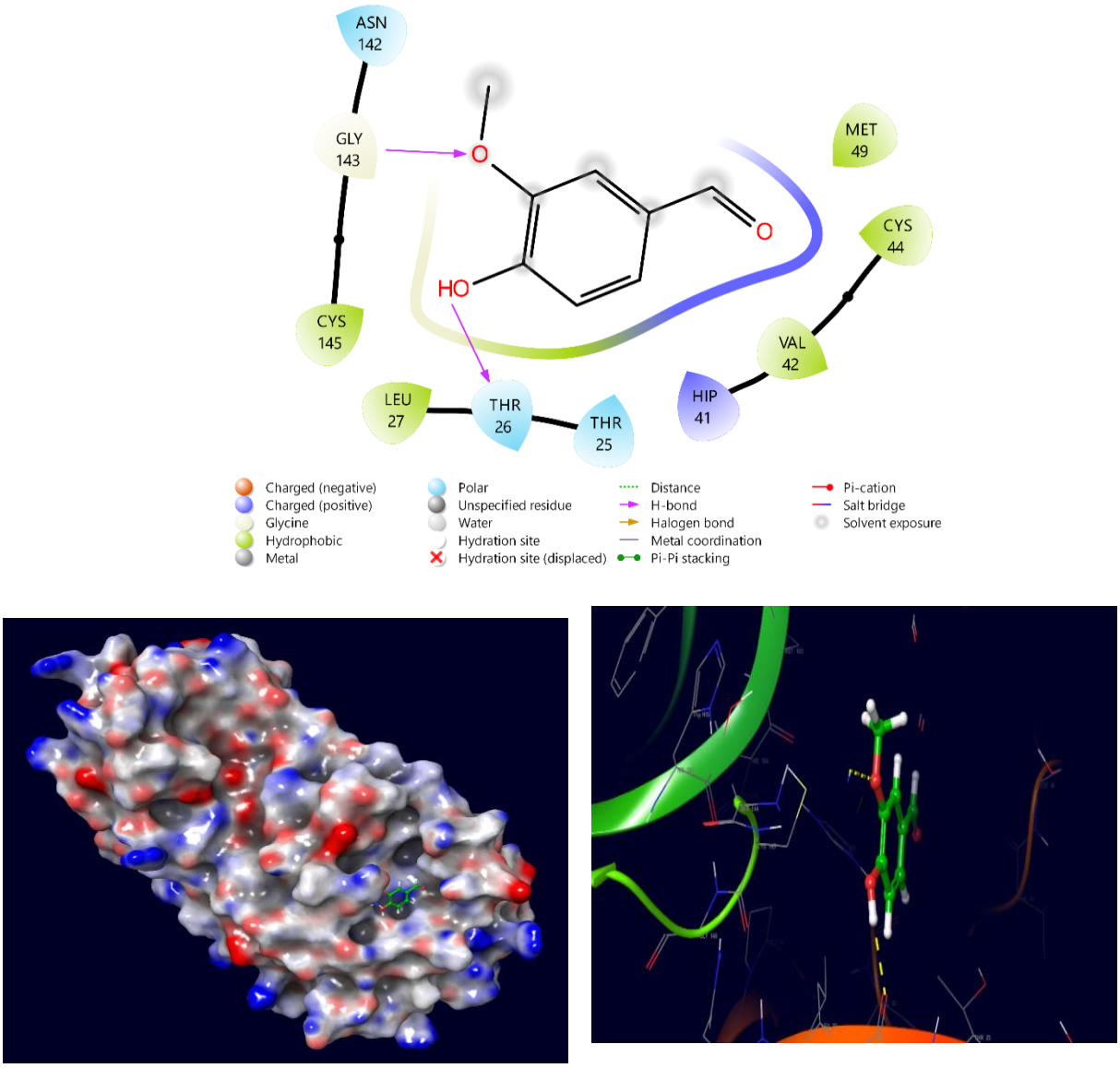

Figure 2. 2D and 3D docking interactions depicting the binding pose of vanillin (ligand) within the active site of SARS-CoV-2 3CL-protease (PDB ID: 9LVV). Hydrogen bonds and interacting residues are emphasized.

4.1.2 Thiosemicarbazide

Docking of thiosemicarbazide, based on the results, showed that it had a relatively weak binding affinity toward the 3CL-protease active site (docking score of –3.311 kcal/mol). The ligand formed hydrogen bonds with Glu166 and Phe140 and the sulfur atom pointed toward His163 and Met165 residues in the binding pocket. Though these interactions were formed, the molecule also showed very few hydrophobic contacts and did not fully occupy the catalytic cleft surrounding Cys145 and His41 (Figure 3). This indicates that thiosemicarbazide has a low level of inhibitory action against 3CL-protease compared with vanillin and its derivative.

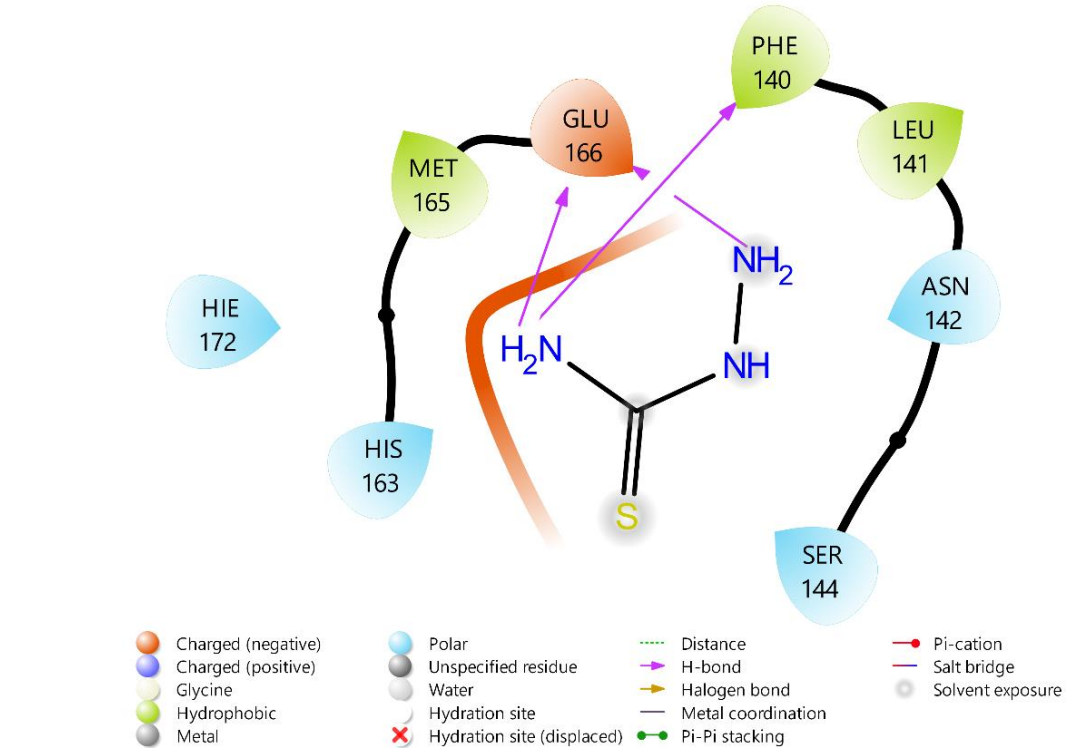

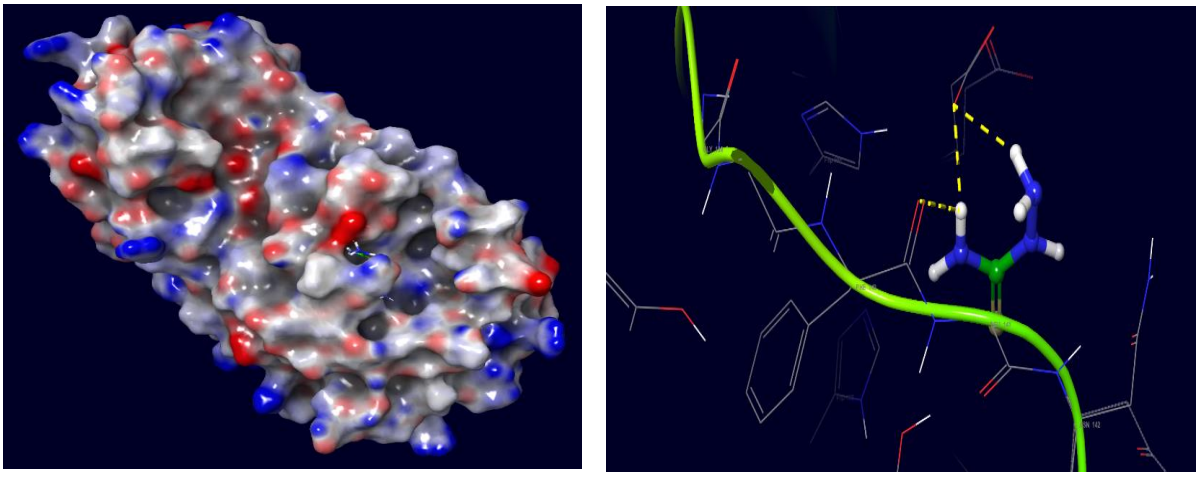

Figure 3. 2D and 3D docking interactions depicting the binding pose of thiosemicarbazide (ligand) within the active site of SARS-CoV-2 3CL-protease (PDB ID: 9LVV). Hydrogen bonds and interacting residues are emphasized.

4.1.3 VTSC

The molecular docking study exhibited docking score of VTSC with SARS-CoV-2 3CL-protease -4.99 kcal/mol and which corresponds to its favourable binding within active site. The compound shown in Figure 4 is properly fitted inside the pocket with interactions to active site residues at the active site for its stabilization. Hydrogen-bond interactions were observed with Glu166, His164 and others which are critical to substrate recognition and stabilization within the protease active site. The ligand's binding stability and orientation were also aided by hydrophobic interactions with other residues such as Met165, Leu141 and Phe140. The overall negative docking score and the interaction pattern presented in Figure 4 reveal that VTSC can be a potent inhibitor candidate against SARS-CoV-2 3CL-protease.

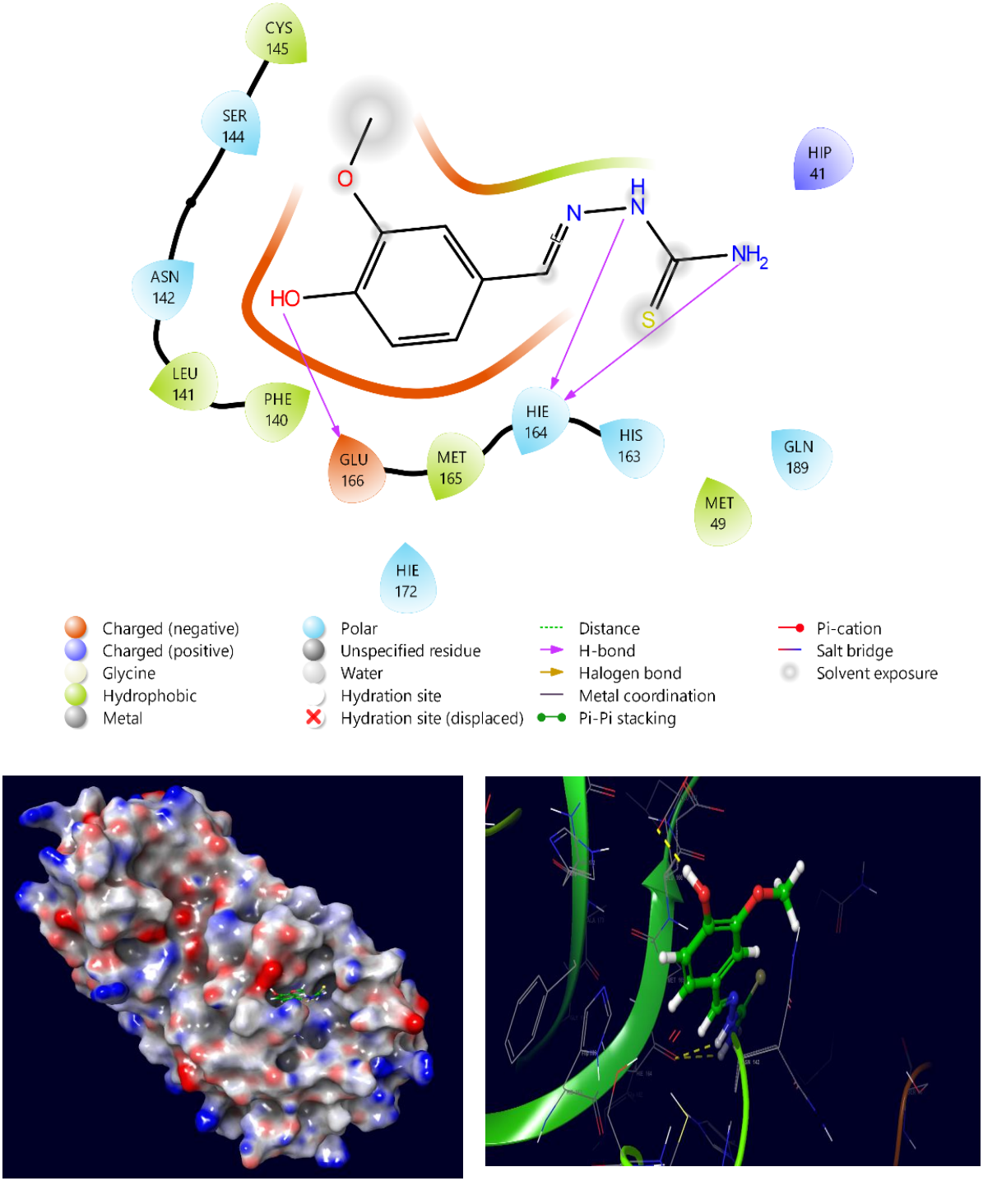

Figure 4. 2D and 3D docking interactions showing the binding pose of VTSC within the active site of SARS-CoV-2 3CL-protease (PDB ID: 9LVV). Hydrogen bonds and interacting residues are highlighted.

4.1.4 Overall Docking Evaluation

The docking study showed that VTSC has the most favorable binding energy and interaction profile within the 3CL-protease active site, followed by vanillin, whereas thiosemicarbazide alone displayed the weakest affinity. VTSC works better because the vanillin ring connects better with the thiosemicarbazone. Together they provide more contact (hydrogen-bonding, π–π, hydrophobic) which fit them better into the enzyme binding pocket. Thanks to these results, it is suggested that the covalent linkage of vanillin to the thiosemicarbazone core stabilizes the resulting molecule and confers an exquisite specificity that translates into greater potency compared with either precursor (Table 2).

Table 2. Comparative docking scores and inferred binding strength of VTSC, vanillin, and thiosemicarbazide against SARS-CoV-2 3CL-protease.

Compound	**Docking Score (kcal/mol)**	**Inferred Binding Strength**
Vanillin–Thiosemicarbazone	–4.99	Good
Vanillin	–4.764	Moderate
Thiosemicarbazide	–3.311	Weak

4.2 FT-IR Spectral Characterization of VTSC

The FT-IR spectra for VTSC experiment (Figure 5) showed the major bands as expected from the vanillin–thiosemicarbazone scaffold design. The wide band around ≈3350 cm^{-1} is due to overlapping O–H and N–H stretching vibrations, indicating phenolic and thiosemicarbazide NH groups. An indelible band at ≈1600 cm^{-1}, which was associated with the azomethine C=N stretch, is assigned to a successful condensation between the vanillin and thiosemicarbazide. Further bands at ≈1550 cm^{-1} (aromatic C=C), ≈1240 cm^{-1} (C–O–C of the methoxy group) and ≈770 cm^{-1} (C=S of the thioamide moiety) are in agreement with the proposed structure and favor the formation of the VTSC ligand instead of a combination of the starting materials.

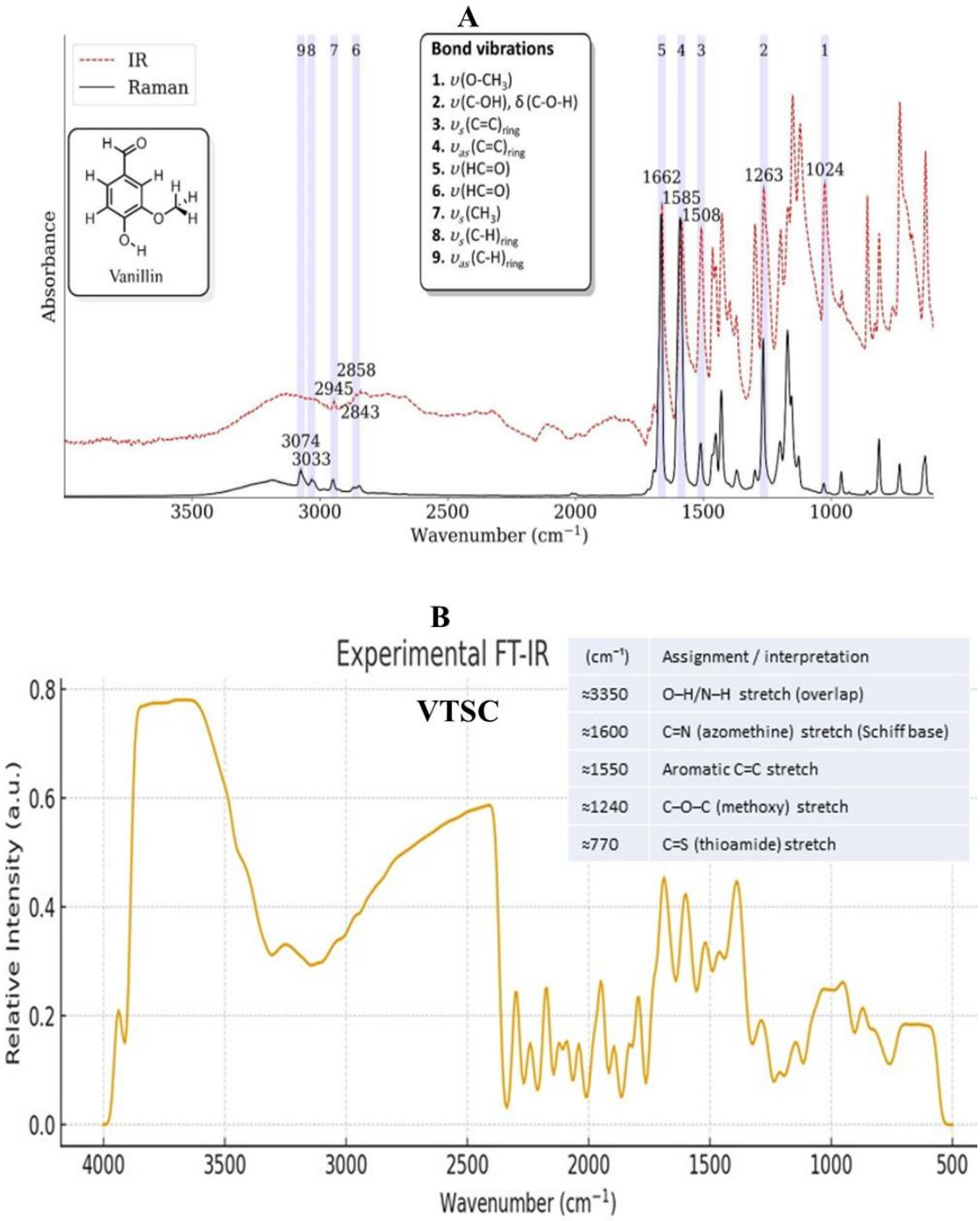

Figure 5. FT-IR spectra of **(A)** vanillin (Nicolaou et al., 2023) and **(B)** vanillin–thiosemicarbazone (VTSC). Compared with vanillin, VTSC shows the disappearance of the aldehydic C=O band and the appearance of characteristic C=N (azomethine) and C=S

(thioamide) bands, confirming successful Schiff base formation and incorporation of the thiosemicarbazone moiety.

4.3 In Vitro 3CL-protease Inhibition and Dose–Response Analysis

4.3.1 Normalized dose–response curve of vanillin against SARS-CoV-2 3CL-protease

Vanillin inhibited SARS-CoV-2 3CL-protease in a clear dose-dependent manner (Figure 6). According to the data, the IC_{50} value of ≈42.0 µM (95% CI 33–54 µM) with the observed inhibition being statistically significant *($p < 0.05$)*. The curve demonstrates that the protease activity decreases gradually as the concentration of vanillin increases, indicating moderate inhibitory potency of vanillin in the tested concentration range.

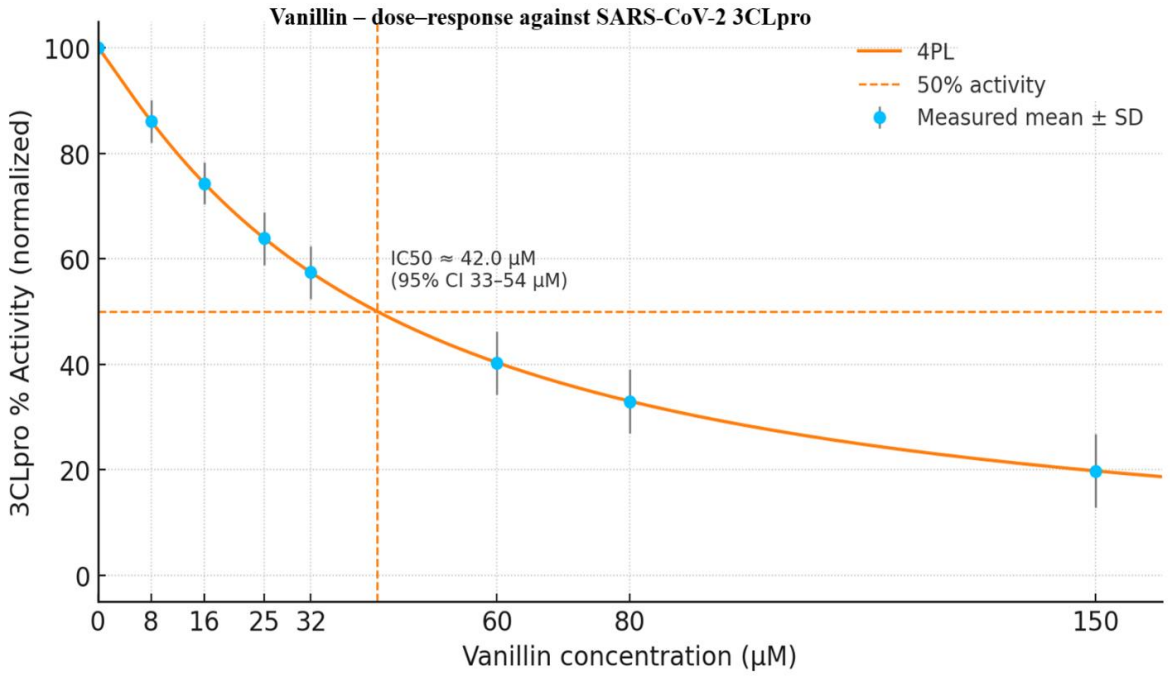

Figure 6. Normalized dose–response curve of vanillin against SARS-CoV-2 3CL-protease. Data are mean ± SD (n = 3) fitted with a 4-parameter logistic (4PL) model. The calculated IC_{50} is ≈42.0 µM (95% CI: 33–54 µM), with the observed inhibition being statistically significant *($p < 0.05$)*.

4.3.2 Normalized Dose–response curve of thiosemicarbazide against SARS-CoV-2 3CL-protease

Thiosemicarbazide displayed a weaker inhibitory profile against 3CL-protease (Figure 7). The 4PL fit (top fixed at 100% activity) gave an IC_{50} of ≈191 µM (95% CI 168–218 µM) however, there was no statistically significant inhibitory effect observed. *($p > 0.05$).* The activity of this enzyme was high at lower and intermediate concentrations and only fell at higher doses. This is consistent with thiosemicarbazide being a low-affinity inhibitor under the assay conditions used.

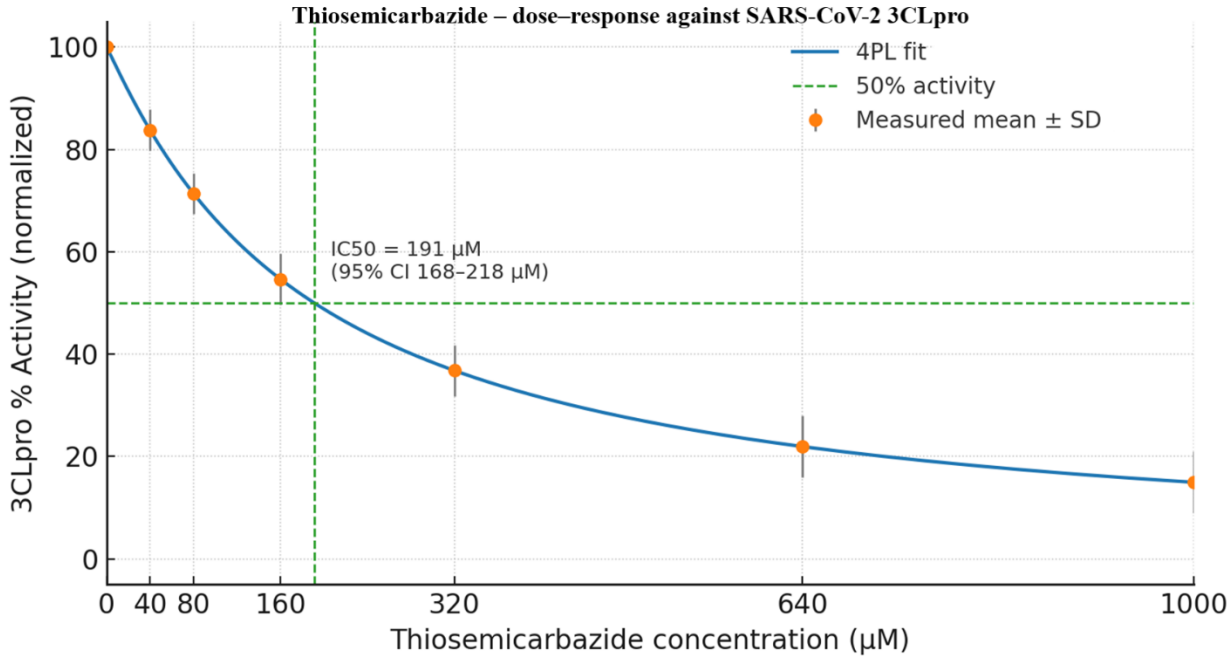

Figure 7. Normalized Dose–response curve of thiosemicarbazide against SARS-CoV-2 3CL-protease. Normalized % activity (mean ± SD, n = 3) was fitted with a 4PL model, giving an IC_{50} of ≈191 µM (95% CI: 168–218 µM), indicating weak inhibition; there was no statistically significant inhibitory effect observed. *($p > 0.05$).*

4.3.3 Normalized Dose–response curve of VTSC against SARS-CoV-2 3CL-protease

In contrast, the hybrid Vanillin–Thiosemicarbazone ligand (VTSC) showed a markedly enhanced effect on 3CL-protease inhibition (Figure 8). The 4PL model fitted to % inhibition data yielded an IC_{50} of ≈28.7 µM (95% CI 25.5–32.6 µM), lower than that of either vanillin or thiosemicarbazide alone with statistically significant inhibition *($p < 0.05$)*. This leftward shift of the curve indicates that covalent linkage of the vanillin and thiosemicarbazide pharmacophores improves overall potency, consistent with the docking results suggesting more favorable and cooperative binding interactions within the protease active site.

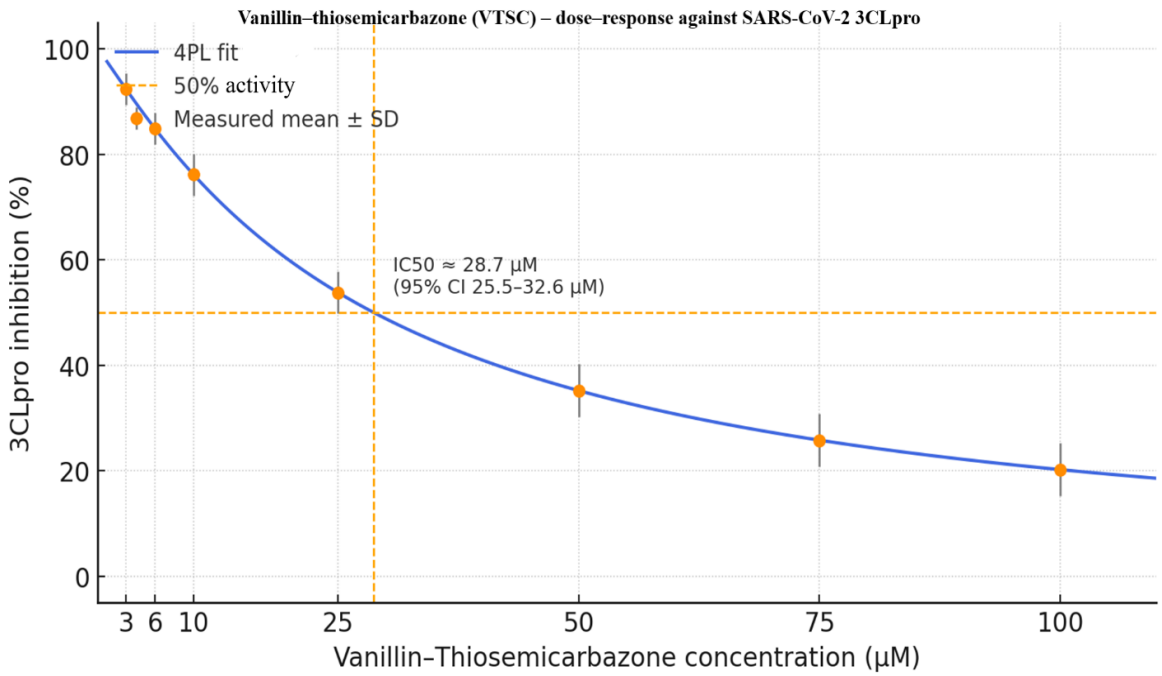

Figure 8. Normalized Dose–response curve of VTSC against SARS-CoV-2 3CL-protease. Points represent mean ± SD (n = 3). A 4PL fit yielded an IC_{50} of ≈28.7 µM (95% CI: 25.5–32.6 µM), showing improved potency compared with either parent compound, with statistically significant inhibition *($p < 0.05$)*.

4.3.4 Comparative Interpretation

Collectively, the in vitro inhibition data demonstrate the following order of potency against SARS-CoV-2 3CL-protease:

VTSC (IC_{50} ≈ 28.7 μM) > vanillin (IC_{50} ≈ 42.0 μM) >> thiosemicarbazide (IC_{50} ≈ 191 μM).

The results indicate a stronger binding affinity between the vanillin core and thiosemicarbazone moiety to the active site of 3CL-protease, which improves binding interaction. The better binding interaction of the molecule was translated into higher inhibitory activity. VTSC thus emerges as a more promising candidate scaffold than either of its parent compounds for further optimization as a potential SARS-CoV-2 3CL-protease inhibitor.

Chapter Five

Discussion

5.1 Overview of Key Findings

In this work, we synthesized and spectroscopically verified vanillin–thiosemicarbazone (VTSC), performed molecular docking to test its interaction with the SARS-CoV-2 3CL-protease, and measured enzyme inhibition with a validated fluorometric assay. Overall, across all readouts, VTSC was superior to its parent compounds, docking ranked VTSC (–4.99 kcal/mol) > vanillin (–4.764 kcal/mol) ≫ thiosemicarbazide (–3.311 kcal/mol), and the IC_{50} values reflected this order (≈28.7 μM < ≈42.0 μM ≪ ≈191 μM). FT-IR supported successful Schiff-base formation (diagnostic C=N), supporting the use of a hybrid scaffold and supporting the interpretation of activity was not attributed to residual starting materials (Czylkowska et al., 2024; Swaminathan et al., 2023). The directional correspondence of in silico ranking with enzyme potency (obtained under matched assay conditions with on-plate GC-376 control and DMSO ≤1%), supports the internal validity of the results and suggests that covalently linking a vanillin core to a thiosemicarbazone pharmacophore enhances the complementarity to the 3CL-protease binding pocket which, in the present assay setting, leads to measurable improvements in inhibitory potency (BPS Bioscience, n.d.; Le Berre et al., 2022; Kuzikov et al., 2021). In practice, VTSC presents itself as a straightforward, synthetically available lead with a distinct advantage over vanillin and thiosemicarbazide and justifies a structural optimization to target more depth in occupancy of S2/S4 subsites and enhanced hydrogen bonding in the catalytic cleft, while further kinetics, cellular, and selectivity studies focus on mechanism and developability (Zagórska et al., 2024; Banerjee et al., 2024).

5.2 Interpretation of Docking Results

On docking, 3 ligands were localized in the substrate-binding cleft of the 3CL-protease and repeatedly associated with Glu166, His163/His164, Gly143, Thr26, Met165, Phe140, and the catalytic dyad His41–Cys145 as the most prominent interaction partners, which are consistently found to coordinate ligand recognition and catalysis in this enzyme (Zagórska et al., 2024; Banerjee et al., 2024). In this best-ranked of the poses, VTSC formed

a denser and more cooperative interaction network than either parent compound: it bound multiple hydrogen bonds to Glu166 and His163/His164 that immobilized the ligand at the S1/S1′ region, and π/alkyl contacts with Phe140 and Met165 promoted the aromatic core and stabilized it further in the pocket of the scaffold; the VTSC also approached Cys145 in a geometry compatible with the successful occupation of the catalytic cleft. Vanillin, in contrast, formed fewer hydrogen bonds (e.g., Thr26, Gly143), less penetrative into the hydrophobic cavity, and less permissive contacts overall, and did not position stably close to the dyad. The cumulative effect is that VTSC has the most effective occupancy of S1/S1′/S2/S4 and there is an apparent structural rationale for its better predicted affinity and observed potency (Zagórska et al., 2024; Banerjee et al., 2024).

At the functional level, VTSC's azomethine (C=N) and thiosemicarbazone (C=S / NH) motifs give directional donors and acceptors corresponding to the polar architecture represented by Glu166 and histidines in S1, whilst the phenolic/methoxy-substituted ring gives π-surface well adapted for the interactions with Phe140/Met165. The mixed polar-aromatic complementarity is less achievable for each parent and leads to the more favorable scoring although the raw docking energy difference is relatively small. Crucially, the image placed VTSC alongside His41–Cys145, suggesting either competitive or mixed binding in the substrate, an assumption subject to kinetic validation (Zagórska et al., 2024; Banerjee et al., 2024).

Mechanistically, the rank-order concordance of docking and enzyme inhibition may be read as more qualitative evidence than as an explicit quantitative prediction: the docking approach is to treat the enzyme predominantly as a fixed receptor, simplifies solvation and protonation states and it ignores the role of water-mediated bridges that can be very relevant near Glu166/Gly143. Notwithstanding these limitations, the repeated contacts as mentioned above closely approximate the structural details of 3CL-protease and are consistent with the mechanistic evidence for the enhanced activity of VTSC in relation to vanillin and thiosemicarbazide (Zagórska et al., 2024; Banerjee et al., 2024).

5.3 Structure–Activity Relationship (VTSC vs Parents)

Three potential elements may account for the advantageous design of VTSC: (i) the azomethine (C=N) linkage that adds a directional hydrogen-bonding vector, favoring partial planarity/conjugation along the scaffold; (ii) the thiosemicarbazone fragment (C=S with dual NH donors), which generates donor/acceptor density and facilitates soft-site interactions in polar pockets; (iii) the phenolic/methoxy-substituted benzaldehyde core which provides a π-surface for stacking plus auxiliary hydrogen bonding through the phenolic OH and methoxy oxygen (Md Yusof et al., 2019& Akitsu et al., 2024). Together, these properties increase the ligand's interaction repertoire toward residues that stabilize the S1/S1′ region (e.g., Glu166, His163/His164); and to promote other π/alkyl contacts deeper in S2/S4 (e.g., Phe140, Met165) which the two parents are hardly capable of satisfying. From an operational standpoint, this mixed polar–aromatic complementarity partly accounts for the left-shift for VTSC in dose–response studies (lower IC_{50} vs vanillin and thiosemicarbazide) and for better geometric/electronic match to the 3CL-protease binding cleft and greater stability of the occupancy of catalytically relevant subsites (Arya et al., 2021; Kafali et al., 2024; Czylkowska et al., 2024; Veg et al., 2025).

In addition, the C=N linkage extends π-conjugation of the aromatic ring with the thiosemicarbazone moiety, decreasing rotational freedom and enabling poses that allow for hydrogen-bond vectors to be maintained to Glu166/His163 whilst keeping the ring most optimally oriented to Phe140/Met165 contacts. The thioamide (C=S), which is a softer acceptor than a typical carbonyl, may improve compatibility with the microenvironment of S1′, thus stabilizing the interaction near Cys145. Finally, depending on local protonation the phenolic OH may act as a conditional donor/acceptor providing a form of pose plasticity that the parent aldehyde (vanillin) is unable to achieve after leaving the thiosemicarbazone framework, and thus may explain why the hybrid achieves a denser and more persistent network of interaction than either precursor (Arya et al., 2021; Kafali et al., 2024; Czylkowska et al., 2024; Veg et al., 2025; Xiao et al., 2024; Mushebenge et al., 2024).

5.4 Correlation Between Docking and in Vitro Inhibition

The qualitative agreement among the docking rank order (VTSC > vanillin ≫ thiosemicarbazide) and experimentally determined IC_{50} values reinforces the internal validity of the approach, and is in agreement to reports in previous work in which ligands of similar size and polarity are screened under controlled protocol conditions (Le Berre et al., 2022; Kuzikov et al., 2021; Fagnani et al., 2024; Zhu et al., 2020).

In this situation, docking-based interaction schedules (e.g., the anchoring at Glu166/His163–His164 and occupancy of S1/S2/S4) often match relative potency differences discovered in laboratory fluorometric enzyme assays even when absolute docking energies do not map linearly into IC_{50} magnitudes (Kuzikov et al., 2021; Fagnani et al., 2024). Some numerical differences between expected binding energies and measurements of experimental potencies are anticipated because of typical docking: (i) receptor is assumed to be a rigid system in general, (ii) solvation/protonation/tautomer equilibria are simplified and easy (especially at His41/His164), and (iii) water-mediated bridges are under modeled around Glu166/Gly143 – all modulating actual binding free energies and kinetic output (Kuzikov et al., 2021; Fagnani et al., 2024). However, the enzyme assay incorporates induced fit contributions, the microenvironmental water, and the entropic effects encoded in the measured inhibition curve that have been only crudely approximated by the scoring functions (Le Berre et al., 2022; Kuzikov et al., 2021).

Methodologically, the consensus evident for all three ligands was explained in several ways here: (1) all three ligands were docked with the same parameters against the same 3CL-protease structure (preserving comparability of scores and poses), (2) inhibition was measured in a single kit format, with a fixed substrate sequence and concentration, as well as constant DMSO ≤1%, limiting protocol-driven variance; and (3) the concentration–response data were modeled into 4PL nonlinear regression of 95% confidence intervals, to insure that the rank order represents true separation of the curves rather than noise (Le Berre et al., 2022; Kuzikov et al., 2021; Zhu et al., 2020). Together, both these controls mitigate typical confounders (e.g., substrate-competition artifacts, signal window compression or plate-to-plate drift) and yield the directional match an increased docking interaction effect for VTSC

accompanied by a left-shifted inhibition curve which is mechanistically plausible (Le Berre et al., 2022; Kuzikov et al., 2021; Fagnani et al., 2024; Zhu et al., 2020).

Docking, therefore, is a structural hypothesis generator on the one hand, whereas enzyme assay is the quantitative arbiter; their convergence for VTSC versus its parents reinforces the conclusion that the hybridization of the vanillin core with a thiosemicarbazone motif yields a ligand, its interaction network in the 3CL-protease cleft plausibly explaining its improved inhibitory potency under the tested conditions (Le Berre et al., 2022; Kuzikov et al., 2021; Fagnani et al., 2024; Zhu et al., 2020).

5.5 FT-IR Evidence Supporting VTSC Formation

The FT-IR spectrum showed a C=N (azomethine) peak at around 1600 cm^{-1}, a C=S (thioamide) peak at around 770 cm^{-1}, and a broad O–H/N–H envelope at about 3350 cm^{-1}, with aromatic and methoxy peaks observed at 1550 and 1240 indicative of the intended thiosemicarbazone, not a physical admixture of the starting constituents (Czylkowska et al., 2024; Swaminathan et al., 2023). This spectroscopic confirmation grounds the biological interpretation specifically to the hybrid scaffold.

5.6 Quantitative Analysis of Dose–Response and IC_{50}

The concentration–response data (% activity or % inhibition against $\log_{10}$[compound]) were analysed with a four-parameter logistic (4PL, variable-slope) model—appropriate for a priori unknown plateaus and unknown Hill slope. We used GraphPad Prism to conduct the fits, fixing the top at 100% response while leaving the bottom free to account for the potential of incomplete inhibition under our assay conditions. We then estimated the hill slope from the data for each of our compounds (Le Berre et al., 2022). Replicate analyses (n = 3 per concentration) were performed separately, and residual diagnostics (random scatter, no curvature, no systematic trends across concentrations) demonstrated sufficient model adequacy. If the variance of measurements was elevated at higher concentrations, a standard least-squares fit was checked against robust regression analysis to verify the stability of parameter estimates, and those results were concordant (Le Berre et al., 2022; Kuzikov et al., 2021).

Under these conditions, VTSC yielded a lower IC_{50} than vanillin, with both clearly separated from thiosemicarbazide. The nonlinear regression statistical results (asymptotic analysis based on Prism) yielded 95% confidence intervals (CIs), and the fit to the curve was checked by R^2, residual plots, and information criteria (AIC), so that no over-parameterization was considered for the dynamic range (Le Berre et al., 2022; Kuzikov et al., 2021). The micromolar IC_{50} range observed for VTSC (≈28.7 μM), with vanillin and thiosemicarbazide showing weaker inhibition, falls within the general low- to mid-micromolar window reported for many early-stage non-peptidic small-molecule SARS-CoV-2 3CL-protease inhibitors evaluated in similar recombinant fluorometric assays (Xiao et al., 2024; Braconi et al., 2025). To check for cross-category differences like CI overlap, a one-way ANOVA was conducted, with Tukey's post hoc test, of % inhibition at matched concentrations as an orthogonal check to complement IC_{50} analysis. We also used an extra-sum-of-squares F-test (global fit of shared versus separate curves). This was used to provide statistically valid assurance as to how well the compounds can share the same 4PL parameters (top/bottom versus slope). Separate curves were preferred (Le Berre et al., 2022; Kuzikov et al., 2021; Zhu et al., 2020)., due to distinct pharmacodynamic profiles.

Collectively, such approaches echo the best practice for nonlinear regression of inhibitory responses: constrain only biologically sensible parameters (the top), check the assumptions of the model by inspection of residuals, calculate IC_{50} with 95% CIs, compare the effect sizes at fixed doses, and employ global model tests with multiple curves. Consistent with statistical and methodological evidence, according to the present assay conditions, VTSC (≈28.7 μM) < vanillin (≈42.0 μM) ≪ thiosemicarbazide (≈191 μM) is statistically and methodologically well supported [14,15,23] (Le Berre et al., 2022; Kuzikov et al., 2021; Zhu et al., 2020).

5.7 Assay Validity and Benchmarking

Use of a commercial, plate-based 3CL-protease fluorometric kit with a defined FRET substrate (DABCYL–KTSAVLQSGFRKME–EDANS) and GC-376 as an on-plate reference inhibitor for standardization on step-by-step procedure and internal verification throughout runs (Trott & Olson, 2010; Braconi et al., 2025). Standard DMSO ≤1% (v/v), triplicates (n =

3), background conditions (no enzyme-controlling) and fixed readout values (Ex 336 nm / Em 455–460 nm) are the requirements for the reliability and interpretability aspects of early enzyme screening and reduce solvent and optics artifacts (BPS Bioscience, n.d.; Le Berre et al., 2022; Kuzikov et al., 2021).

Plates were mechanically monitored in the linear step towards reaction progress (time window confirmed verifier by a pilot read) and the vehicle (DMSO) wells were normalized to 100% activity and the background signal removed prior to % inhibition determination. Assay quality was assessed through (i) ensuring a proper signal window (mean signal-to-background ratio > 5–10), (ii) limiting replicate variability (low coefficient of variation on control wells), and (iii) confirming clear separation between positive (GC-376) and negative (vehicle) controls across runs (BPS Bioscience, n.d.; Le Berre et al., 2022; Kuzikov et al., 2021; Fagnani et al., 2024; Zhu et al., 2020). The use of black plates and matched DMSO in each well prevented inner-filter and compound autofluorescence, and all compound-only wells (where no substrate was used) were inspected to rule out optical interference. This guidance is consistent with manufacturer recommendations for the 3CL-protease kit and general guidance regarding fluorometric inhibition assays (BPS Bioscience, n.d.; Le Berre et al., 2022; Kuzikov et al., 2021). To enable assessment of the assay's reliability and reproducibility, GC-376 was introduced on all plates; while IC_{50} values for GC-376 differ for each protocol and enzyme build it is always shown in the sub-micromolar range against 3CL-protease in the literature, and a robust positive control than first pass, simple scaffolds like VTSC (Kuzikov et al., 2021; Zhu et al., 2020).

Accordingly, the micromolar activity of VTSC can be considered as internally consistent in this validated format of study and cross-study numerical comparisons are based on the substrate sequence and concentration, enzyme batch, buffer conditions, and readout time. Combined, the standardization of the kits, and integration of on-plate control and statistical curve fitting (4PL with 95% CIs) further supports the robustness of the potency ranking acquired in this work (BPS Bioscience, n.d.; Le Berre et al., 2022; Kuzikov et al., 2021; Zhu et al., 2020).

5.8 Putative Mode of Inhibition

The position of VTSC in the substrate-binding pocket of the 3CL-protease (anchored by hydrogen bonds to Glu166 and His163/His164, and positioned proximal to the His41–Cys145 catalytic dyad and the oxyanion loop (Gly143–Ser144–Cys145)) is best considered a competitive association at the substrate site, with the caveat that a mixed component cannot be excluded based solely on docking (Zagórska et al., 2024; Banerjee et al., 2024; Veg et al., 2025).

The interaction pattern follows the canonical S1/S1′/S2/S4 subsites used by substrate-like ligands, and as for the present conditions, VTSC has no clear electrophilic "warhead" for covalent bond formation to Cys145, revealing a non-covalent reversible mechanism (Zagórska et al., 2024; Banerjee et al., 2024; Veg et al., 2025). To establish the competitive vs. mixed inhibition distinction experimentally with the right models the kinetic analyses are needed at different substrate concentrations ([S]), fitting global models to derive Ki (or αKi for the mixed models), and examining the characteristic alteration in Vmax and Km with a single competitive inhibitor enhancing the apparent Km (rightwards shifts the Michaelis–Menten curve), while a mixed inhibitor perturbs both parameters in a concentration-dependent manner (Le Berre et al., 2022; Kuzikov et al., 2021; Mushebenge et al., 2024). Complementary diagnostics include global extra-sum-of-squares F-tests contrasting competitive, non-competitive, and mixed models, and time-course assessments of time-dependent inhibition (e.g., progress-curve analysis) to rule out slow-binding artifacts that may disguise as mixed behavior (Le Berre et al., 2022; Kuzikov et al., 2021; Mushebenge et al., 2024). Overall, structural evidence (subsite occupancy, dyad proximity, and lack of a covalent warhead) presents a competitive-based hypothesis about VTSC while definitive mechanistic assignment remains for global kinetic fitting over varied [S] to segment effects on Km and Vmax and appropriately quantify Ki (±α) (Le Berre et al., 2022; Zagórska et al., 2024; Banerjee et al., 2024; Xiao et al., 2024; Mushebenge et al., 2024).

5.9 Selectivity Considerations (Conceptual)

Since there are no closely homologous forms of the 3CL-protease, the enzyme is considered a selective antiviral target at the enzyme level (Zagórska et al., 2024; Banerjee et al., 2024). Nevertheless, selectivity should be shown from an objective standpoint: early triage should contain counterscreens against representative human proteases (e.g., cysteine and serine proteases) and common off-targets as well as straightforward cytotoxicity profiling. This may be especially the case for thiosemicarbazone scaffolds, which exhibit a plurality of hydrogen-bond donors and acceptors and may bind to the unwanted polar sites (Czylkowska et al., 2024; Veg et al., 2025). In this respect, a preliminary selectivity window is necessary prior to further developments of VTSC (Veg et al., 2025; Mushebenge et al., 2024).

5.10 Methodological strengths

The major merits of this work are:

(i) orthogonal pipeline–spectroscopic confirmation → docking → enzyme inhibition giving convergent evidence; (ii) matched docking parameters between ligands, ensuring fair pose/score comparisons; (iii) standardized assay conditions with an internal positive control (GC-376) and balanced solvent concentrations (DMSO ≤1%); and finally (iv) statistically principled nonlinear regression (4PL) with 95% confidence intervals (CIs) and orthogonal checks (ANOVA/Tukey; optional extra-sum-of-squares tests) (BPS Bioscience, n.d.; Le Berre et al., 2022; Kuzikov et al., 2021; Zhu et al., 2020). All those ingredients together constitute a coherent evidentiary chain that establishes a framework to underpin the central conclusions of the study.

5.11 Limitations

Results are restricted to a purified enzyme context alone, and do not account for cellular permeability, metabolic stability, or antiviral efficiency in replicating systems. Docking is based on a highly rigid receptor and a simplified solvation/protonation model whose molecular dynamics (MD) simulations will be needed to evaluate the stability of the

pose and the water-mediated contacts over time (Zagórska et al., 2024; Xiao et al., 2024; Mushebenge et al., 2024). Only one hybrid (VTSC) and two parents were profiled; wider structure–activity relationship (SAR) study might identify activity cliffs and more promising analogues. Neither counterscreens/selectivity assays nor mechanistic kinetics (Km, competitive vs. non-competitive/mixed) were conducted, with mode of inhibition and off-target danger remaining a major focus for future work (Kuzikov et al., 2021; Xiao et al., 2024; Mushebenge et al., 2024).

5.12 Implications for Lead Optimization

However, VTSC demonstrates that straightforward hybridization can obtain a measurable gain in 3CL-protease inhibition. Docking poses and subsite topography suggest several tractable modifications:

• Balancing polarity of phenolic O-substitution in ethers or bioisosteres by deeper S2/S4 occupancy.

• Modulating C=N electronics (para/meta substituents) to refine hydrogen-bond directionality toward Glu166/His163 and optimize pose stability.

• Probing thioamide variants (thioamide → amide/thiourea analogues) to test compatibility with S1/S1′ and mitigate potential liabilities.

• Introducing small hydrophobic or heteroaryl appendages to reinforce π/alkyl contacts with Phe140/Met165 and expand S2/S4 engagement, mirroring design cues from non-peptidic series (Banerjee et al., 2024; Xiao et al., 2024; Braconi et al., 2025).

All proposals are synthetically accessible from the vanillin platform and amenable to rapid SAR cycles (Arya et al., 2021; Kafali et al., 2024; Veg et al., 2025; Braconi et al., 2025).

5.13 Future Work

Immediate next steps include: (1) MD simulations (100–200 ns) for VTSC and vanillin complexes to quantify RMSD/RMSF and water-bridge persistence; (2) enzyme

kinetics at different substrate levels for mode and Ki (±α for mixed models); (3) cell-based antiviral assays (e.g., replicon or cytopathic-effect reduction) in combination with cytotoxicity for selectivity indices; (4) initial in vitro ADME (solubility, microsomal stability, PAMPA/Caco-2) to gauge developability; (5) a focused analogue set varying phenolic substitution and thiosemicarbazone electronics to establish SAR and potency ceilings. It is important to consider 3CL-protease mutations in the design of resistance-proof drugs (Xiao et al., 2024; Mushebenge et al., 2024; Braconi et al., 2025).

Conclusion

For this study, Vanillin–Thiosemicarbazone (VTSC) has been synthesized and structurally validated then utilized as an inhibitor of SARS-CoV-2 3CL-protease via an integrated molecular docking and in vitro fluorometric assay protocol. VTSC docked better and exhibited lower IC_{50} than its parent compounds vanillin and thiosemicarbazide. The hybridization of thiosemicarbazone pharmacophore on the vanillin core increased its complementarity to the 3CL-protease active site, thereby enhancing its inhibitory activity. VTSC could serve as a convenient and synthetic lead scaffold for further structure–activity optimization and mechanistic studies according to these results. Further work, including detailed enzyme kinetics, cellular antiviral assays, selectivity profiling and first ADME analysis is essential to assess whether VTSC or its analogues could go into advanced preclinical development.

References

Akitsu, T., Nakane, D., & Miroslaw, B. (2024). Viewpoints Concerning Crystal Structure from Recent Reports on Schiff Base Compounds and Their Metal Complexes. Symmetry, 16(11), 1525.

Arya SS, Rookes JE, Cahill DM, Lenka SK. Vanillin: A review on the therapeutic prospects of a popular flavouring molecule. *Advances in Traditional Medicine*. 2021;21(3):1–7.

Banerjee S, et al. Exploring the key structural attributes and chemico-biological interactions of pyridinone-based SARS-CoV-2 3CLpro inhibitors through validated structure-based drug design strategies. *Heliyon*. 2024;10:e40404.

BPS Bioscience. *SARS-CoV-2 3CL Protease Assay Kit – Instruction Manual*. BPS Bioscience, San Diego, CA, USA. Available at: https://www.bpsbioscience.com/

Braconi L, Sosic A, Crocetti L. Recent breakthroughs in synthetic small molecules targeting SARS-CoV-2 Mpro from 2022 to 2024. Bioorganic & Medicinal Chemistry. 2025 May 20:118247.

Czylkowska A, Pitucha M, Raducka A, Fornal E, Kordialik-Bogacka E, Ścieszka S, et al. Thiosemicarbazone-based compounds: A promising scaffold for developing antibacterial, antioxidant, and anticancer therapeutics. *Molecules*. 2024;30(1):129.

Fagnani L, Bellio P, Di Giulio A, Nazzicone L, Iorio R, Petricca S, Franceschini N, Bertarini L, Tondi D, Celenza G. Mechanism of non-competitive inhibition of the SARS-CoV-2 3CL protease dimerization: Therapeutic and clinical promise of the lichen secondary metabolite perlatolinic acid. Heliyon. 2024 Oct 15;10(19).

Froggatt, H. M., Heaton, B. E., & Heaton, N. S. (2020). Development of a fluorescence-based, high-throughput SARS-CoV-2 3CLpro reporter assay. Journal of virology, 94(22), 10-1128.

Hammond, J., Leister-Tebbe, H., Gardner, A., Abreu, P., Bao, W., Wisemandle, W., ... & Rusnak, J. M. (2022). Oral nirmatrelvir for high-risk, nonhospitalized adults with Covid-19. New England Journal of Medicine, 386(15), 1397-1408.

Jin, Z., Du, X., Xu, Y., Deng, Y., Liu, M., Zhao, Y., ... & Yang, H. (2020). Structure of Mpro from SARS-CoV-2 and discovery of its inhibitors. Nature, 582(7811), 289-293.

Kafali M, Finos MA, Tsoupras A. Vanillin and its derivatives: a critical review of their anti-inflammatory, anti-infective, wound-healing, neuroprotective, and anti-cancer health-promoting benefits. *Nutraceuticals*. 2024;4(4):522–561.

Kang C, Foo K, Ethirajulu K, Xu W. An evolving landscape of small molecules targeting SARS-CoV-2: What are we awaiting beyond 3CLpro inhibitors? *Journal of Medicinal Chemistry*. 2025;68(10):9836–9839.

Kronenberger T, Laufer SA, Pillaiyar T. COVID-19 therapeutics: Small-molecule drug development targeting SARS-CoV-2 main protease. *Drug Discovery Today*. 2023;28(6):103579.

Kuzikov M, Costanzi E, et al. Identification of inhibitors of SARS-CoV-2 3CL-pro enzymatic activity using a fluorescence-based assay and 4PL curve fitting. *ACS Pharmacology & Translational Science*. 2021;4(5):1092–1107.

Le Berre, M., Gerlach, J. Q., Dziembała, I., & Kilcoyne, M. (2022). Calculating half maximal inhibitory concentration (IC50) values from glycomics microarray data using GraphPad Prism. In Glycan Microarrays: Methods and Protocols (pp. 89-111). New York, NY: Springer US.

Lv Z, Cano KE, Jia L, Drag M, Huang TT, Olsen SK. Targeting SARS-CoV-2 proteases for COVID-19 antiviral development. *Frontiers in Chemistry*. 2022;9:819165.

Md Yusof, E. N., M. Latif, M. A., M. Tahir, M. I., Sakoff, J. A., Simone, M. I., Page, A. J., ... & BSA Ravoof, T. (2019). o-Vanillin derived Schiff bases and their organotin (IV) compounds: synthesis, structural characterisation, in-silico studies and cytotoxicity. International journal of molecular sciences, 20(4), 854.

Mushebenge AG, Ugbaja SC, Magwaza NN, Mbatha NA, Muzumbukilwa TW, Kadima MG, Tata FY, Nxumalo MB, Manimani RG, Ndage N, Amuri BS. Mechanistic Insights into the Mutational Landscape of the Main Protease/3CLPro and Its Impact on Long-Term COVID-19/SARS-CoV-2 Management. Future Pharmacology. 2024 Nov 28;4(4):825-52.

Nicolaou, M., Senn, H., Gibson, E., & Vilà-Nadal, L. (2023). IR of Vanillin: A classic study with a twist.

Olatunde A, Mohammed A, Ibrahim MA, Tajuddeen N, Shuaibu MN. Vanillin: A food additive with multiple biological activities. *European Journal of Medicinal Chemistry Reports*. 2022;5:100055.

Pacca CC, Marques RE, Espindola JW, Oliveira Filho GB, Leite AC, Teixeira MM, Nogueira ML. Thiosemicarbazones and phthalyl-thiazoles compounds exert antiviral activity against yellow fever virus and Saint Louis encephalitis virus. *Biomedicine & Pharmacotherapy*. 2017;87:381–387.

Padmanabhan P, Khaleefathullah S, Kaveri K, Palani G, Ramanathan G, Thennarasu S, Tirichurapalli Sivagnanam U. Antiviral activity of thiosemicarbazones derived from α-amino acids against dengue virus. *Journal of Medical Virology*. 2017;89(3):546–552.

Razali R, Asis H, Budiman C. Structure–function characteristics of SARS-CoV-2 proteases and their potential inhibitors from microbial sources. *Microorganisms*. 2021;9(12):2481.

Sebaugh, J. L. (2011). Guidelines for accurate EC50/IC50 estimation. Pharmaceutical statistics, 10(2), 128-134.

Swaminathan J, Thennarasu S, et al. Synthesis, geometrical, spectral and antibacterial studies of 4-hydroxy-3-methoxybenzaldehyde thiosemicarbazone by experimental and theoretical investigations. 2023.

Tokalı, F. S., Şenol, H., Katmerlikaya, T. G., Dağ, A., & Şendil, K. (2023). Novel thiosemicarbazone and thiazolidin-4-one derivatives containing vanillin core: Synthesis, characterization, and anticancer activity studies. Journal of Heterocyclic Chemistry, 60(4), 645-656.

Trott, O., & Olson, A. J. (2010). AutoDock Vina: improving the speed and accuracy of docking with a new scoring function, efficient optimization, and multithreading. Journal of computational chemistry, 31(2), 455-461.

Unoh, Y., Uehara, S., Nakahara, K., Nobori, H., Yamatsu, Y., Yamamoto, S., ... & Tachibana, Y. (2022). Discovery of S-217622, a noncovalent oral SARS-CoV-2 3CL protease inhibitor clinical candidate for treating COVID-19. Journal of medicinal chemistry, 65(9), 6499-6512.

Veg E, Hashmi K, Ahmad MI, Joshi S, Khan AR, Khan T. Some Biological Applications and Mechanistic Insights of Benzaldehyde-Substituted Thiosemicarbazones and Their Metal Complexes: A Review. Natural Sciences. 2025 Apr;5(1-2):e70005.

Xiao YQ, Long J, Zhang SS, Zhu YY, Gu SX. Non-peptidic inhibitors targeting SARS-CoV-2 main protease: A review. Bioorganic Chemistry. 2024 Jun 1;147:107380.

Zagórska A, Czopek A, Fryc M, Jończyk J. Inhibitors of SARS-CoV-2 main protease (Mpro) as anti-coronavirus agents. *Biomolecules*. 2024;14(7):797.

Zhu W, Xu M, Chen CZ, Guo H, Shen M, Hu X, Shinn P, Klumpp-Thomas C, Michael SG, Zheng W. Identification of SARS-CoV-2 3CL protease inhibitors by a quantitative high-throughput screening. ACS pharmacology & translational science. 2020 Sep 4;3(5):1008-16.

Appendices I. RAW DATA: FT-IR spectrum (4000–500 cm^{-1})

Wavenumber_cm-1	Relative_Intensity
500	0
506.9034	1.20E-05
513.8067	9.02E-05
520.7101	0.000488
527.6134	0.00206
534.5168	0.006908
541.4201	0.018551
548.3235	0.040338
555.2268	0.072111
562.1302	0.10822
569.0335	0.140198
575.9369	0.162272
582.8402	0.174184
589.7436	0.179291
596.6469	0.181153
603.5503	0.181888
610.4536	0.182378
617.357	0.182907
624.2604	0.183503
631.1637	0.18405
638.0671	0.184387
644.9704	0.184428
651.8738	0.184219
658.7771	0.18394
665.6805	0.183816
672.5838	0.183953
679.4872	0.184267
686.3905	0.184559
693.2939	0.184611
700.1972	0.184057
707.1006	0.182064
714.0039	0.177195
720.9073	0.168058
727.8107	0.154691
734.714	0.139399
741.6174	0.12572
748.5207	0.116314
755.4241	0.111928
762.3274	0.112046
769.2308	0.115868

776.1341	0.122608
783.0375	0.131354
789.9408	0.141061
796.8442	0.150738
803.7475	0.159611
810.6509	0.16703
817.5542	0.172297
824.4576	0.174912
831.3609	0.175507
838.2643	0.176648
845.1677	0.181823
852.071	0.192337
858.9744	0.204964
865.8777	0.213623
872.7811	0.213843
879.6844	0.205414
886.5878	0.191632
893.4911	0.177664
900.3945	0.169335
907.2978	0.171075
914.2012	0.183525
921.1045	0.203294
928.0079	0.225092
934.9112	0.243916
941.8146	0.25635
948.7179	0.261486
955.6213	0.260983
962.5247	0.257591
969.428	0.253448
976.3314	0.249833
983.2347	0.247687
990.1381	0.247298
997.0414	0.247792
1003.945	0.247997
1010.848	0.247842
1017.751	0.248164
1024.655	0.249131
1031.558	0.249372
1038.462	0.246818
1045.365	0.240378
1052.268	0.230964
1059.172	0.220893
1066.075	0.211873
1072.978	0.203276
1079.882	0.19248

1086.785	0.177115
1093.688	0.157257
1100.592	0.13617
1107.495	0.11948
1114.398	0.112703
1121.302	0.117612
1128.205	0.130244
1135.108	0.143232
1142.012	0.150644
1148.915	0.15065
1155.819	0.144434
1162.722	0.133904
1169.625	0.120815
1176.529	0.107296
1183.432	0.096237
1190.335	0.09039
1197.239	0.090475
1204.142	0.093983
1211.045	0.096319
1217.949	0.093849
1224.852	0.086766
1231.755	0.079813
1238.659	0.079884
1245.562	0.091314
1252.465	0.112477
1259.369	0.137221
1266.272	0.159628
1273.176	0.176842
1280.079	0.187954
1286.982	0.192152
1293.886	0.188985
1300.789	0.179672
1307.692	0.167274
1314.596	0.155689
1321.499	0.148689
1328.402	0.149733
1335.306	0.162226
1342.209	0.189014
1349.112	0.230341
1356.016	0.282031
1362.919	0.336434
1369.822	0.38544
1376.726	0.422549
1383.629	0.443544
1390.533	0.447126

1397.436	0.435166
1404.339	0.411747
1411.243	0.381974
1418.146	0.35154
1425.049	0.326235
1431.953	0.310398
1438.856	0.305132
1445.759	0.307893
1452.663	0.313801
1459.566	0.317467
1466.469	0.314599
1473.373	0.304136
1480.276	0.290417
1487.179	0.282073
1494.083	0.286138
1500.986	0.301959
1507.89	0.32121
1514.793	0.333876
1521.696	0.333902
1528.6	0.320468
1535.503	0.296858
1542.406	0.269951
1549.31	0.249589
1556.213	0.245322
1563.116	0.261312
1570.02	0.293852
1576.923	0.33434
1583.826	0.374157
1590.73	0.406139
1597.633	0.423353
1604.536	0.41988
1611.44	0.3945
1618.343	0.353589
1625.247	0.309874
1632.15	0.277102
1639.053	0.264012
1645.957	0.271693
1652.86	0.295576
1659.763	0.329478
1666.667	0.368069
1673.57	0.406366
1680.473	0.437918
1687.377	0.454088
1694.28	0.446079
1701.183	0.411013

1708.087	0.359458
1714.99	0.313325
1721.893	0.287516
1728.797	0.272926
1735.7	0.245898
1742.604	0.195885
1749.507	0.136797
1756.41	0.091898
1763.314	0.076222
1770.217	0.093556
1777.12	0.138721
1784.024	0.194634
1790.927	0.233443
1797.83	0.233507
1804.734	0.199734
1811.637	0.161001
1818.54	0.143064
1825.444	0.145784
1832.347	0.148207
1839.25	0.133024
1846.154	0.102346
1853.057	0.07121
1859.961	0.052484
1866.864	0.051279
1873.767	0.067923
1880.671	0.098096
1887.574	0.129159
1894.477	0.143783
1901.381	0.133954
1908.284	0.110294
1915.187	0.094937
1922.091	0.106454
1928.994	0.149079
1935.897	0.207965
1942.801	0.253974
1949.704	0.26383
1956.607	0.240837
1963.511	0.209363
1970.414	0.186498
1977.318	0.167147
1984.221	0.139102
1991.124	0.102727
1998.028	0.070021
2004.931	0.051592
2011.834	0.051368

2018.738	0.069394
2025.641	0.101302
2032.544	0.133877
2039.448	0.148483
2046.351	0.135969
2053.254	0.106818
2060.158	0.083297
2067.061	0.082313
2073.964	0.104589
2080.868	0.134902
2087.771	0.152998
2094.675	0.150943
2101.578	0.140532
2108.481	0.138862
2115.385	0.147241
2122.288	0.150053
2129.191	0.134922
2136.095	0.108721
2142.998	0.092371
2149.901	0.104441
2156.805	0.14859
2163.708	0.208001
2170.611	0.250538
2177.515	0.249254
2184.418	0.204467
2191.321	0.142616
2198.225	0.092567
2205.128	0.06687
2212.032	0.063892
2218.935	0.078905
2225.838	0.10667
2232.742	0.135817
2239.645	0.149818
2246.548	0.139487
2253.452	0.112155
2260.355	0.085555
2267.258	0.076043
2274.162	0.093668
2281.065	0.139586
2287.968	0.199382
2294.872	0.242893
2301.775	0.242664
2308.679	0.197341
2315.582	0.132299
2322.485	0.076472

2329.389	0.042985
2336.292	0.031046
2343.195	0.03929
2350.099	0.073515
2357.002	0.142013
2363.905	0.243183
2370.809	0.358291
2377.712	0.459981
2384.615	0.529855
2391.519	0.56713
2398.422	0.582361
2405.325	0.586727
2412.229	0.586988
2419.132	0.586074
2426.036	0.585045
2432.939	0.584189
2439.842	0.583441
2446.746	0.582585
2453.649	0.581514
2460.552	0.580336
2467.456	0.579264
2474.359	0.578406
2481.262	0.577645
2488.166	0.576738
2495.069	0.575511
2501.972	0.573958
2508.876	0.572188
2515.779	0.570315
2522.682	0.568413
2529.586	0.566537
2536.489	0.564757
2543.393	0.563166
2550.296	0.561831
2557.199	0.560694
2564.103	0.559556
2571.006	0.558221
2577.909	0.55663
2584.813	0.554847
2591.716	0.552959
2598.619	0.551006
2605.523	0.548974
2612.426	0.546819
2619.329	0.544529
2626.233	0.542176
2633.136	0.539886

2640.039	0.537731
2646.943	0.535697
2653.846	0.533731
2660.75	0.531792
2667.653	0.529853
2674.556	0.527887
2681.46	0.525853
2688.363	0.523698
2695.266	0.521405
2702.17	0.519042
2709.073	0.516713
2715.976	0.514451
2722.88	0.512188
2729.783	0.509859
2736.686	0.507497
2743.59	0.505204
2750.493	0.503046
2757.396	0.501002
2764.3	0.498995
2771.203	0.496938
2778.107	0.494727
2785.01	0.492265
2791.913	0.489474
2798.817	0.486275
2805.72	0.482557
2812.623	0.478235
2819.527	0.473341
2826.43	0.468054
2833.333	0.46266
2840.237	0.457501
2847.14	0.452913
2854.043	0.449074
2860.947	0.445805
2867.85	0.442577
2874.753	0.438855
2881.657	0.434539
2888.56	0.430025
2895.464	0.425758
2902.367	0.421709
2909.27	0.417271
2916.174	0.411722
2923.077	0.404938
2929.98	0.397831
2936.884	0.391957
2943.787	0.388359

2950.69	0.386611
2957.594	0.38509
2964.497	0.382233
2971.4	0.377483
2978.304	0.37125
2985.207	0.364339
2992.11	0.357541
2999.014	0.35155
3005.917	0.346898
3012.821	0.343768
3019.724	0.341863
3026.627	0.34051
3033.531	0.338941
3040.434	0.336548
3047.337	0.333063
3054.241	0.328579
3061.144	0.323411
3068.047	0.317922
3074.951	0.312443
3081.854	0.307323
3088.757	0.302982
3095.661	0.299827
3102.564	0.298006
3109.467	0.2972
3116.371	0.296698
3123.274	0.295843
3130.178	0.294527
3137.081	0.293307
3143.984	0.293013
3150.888	0.294199
3157.791	0.296824
3164.694	0.300304
3171.598	0.303867
3178.501	0.306987
3185.404	0.309639
3192.308	0.31218
3199.211	0.314967
3206.114	0.318071
3213.018	0.321274
3219.921	0.324273
3226.824	0.326861
3233.728	0.328947
3240.631	0.330435
3247.535	0.331117
3254.438	0.330743

3261.341	0.329206
3268.245	0.326653
3275.148	0.323417
3282.051	0.319881
3288.955	0.316436
3295.858	0.313586
3302.761	0.312053
3309.665	0.312663
3316.568	0.31597
3323.471	0.321884
3330.375	0.329656
3337.278	0.338331
3344.181	0.347403
3351.085	0.357217
3357.988	0.3687
3364.892	0.382471
3371.795	0.398045
3378.698	0.41402
3385.602	0.429029
3392.505	0.442402
3399.408	0.454069
3406.312	0.46414
3413.215	0.472708
3420.118	0.479889
3427.022	0.48594
3433.925	0.491358
3440.828	0.497094
3447.732	0.504795
3454.635	0.516462
3461.538	0.533064
3468.442	0.553198
3475.345	0.573609
3482.249	0.591423
3489.152	0.605793
3496.055	0.617585
3502.959	0.628108
3509.862	0.638324
3516.765	0.648738
3523.669	0.659505
3530.572	0.670523
3537.475	0.681548
3544.379	0.692345
3551.282	0.702822
3558.185	0.713052
3565.089	0.723142

3571.992	0.73303
3578.895	0.742443
3585.799	0.751009
3592.702	0.758422
3599.606	0.764564
3606.509	0.769513
3613.412	0.77342
3620.316	0.77636
3627.219	0.778352
3634.122	0.779506
3641.026	0.780054
3647.929	0.780264
3654.832	0.780328
3661.736	0.780344
3668.639	0.780346
3675.542	0.780344
3682.446	0.780331
3689.349	0.78028
3696.252	0.780124
3703.156	0.77975
3710.059	0.779051
3716.963	0.778033
3723.866	0.77688
3730.769	0.775863
3737.673	0.775163
3744.576	0.774789
3751.479	0.774633
3758.383	0.774582
3765.286	0.774569
3772.189	0.774564
3779.093	0.774551
3785.996	0.7745
3792.899	0.774344
3799.803	0.77397
3806.706	0.77327
3813.609	0.772253
3820.513	0.7711
3827.416	0.770082
3834.32	0.769343
3841.223	0.768704
3848.126	0.767194
3855.03	0.761733
3861.933	0.744848
3868.836	0.703746
3875.74	0.625543

3882.643	0.509428
3889.546	0.375479
3896.45	0.25704
3903.353	0.180343
3910.256	0.150611
3917.16	0.155718
3924.063	0.178235
3930.966	0.2017
3937.87	0.210179
3944.773	0.191538
3951.677	0.146723
3958.58	0.091876
3965.483	0.046193
3972.387	0.018443
3979.29	0.005807
3986.193	0.001435
3993.097	0.000277
4000	4.06E-05